

Apoptotic Caspases Suppress mtDNA-Induced STING-Mediated Type I IFN Production

Michael J. White,^{1,5,*} Kate McArthur,^{1,5} Donald Metcalf,^{2,5} Rachael M. Lane,¹ John C. Cambier,⁹ Marco J. Herold,^{4,5} Mark F. van Delft,^{2,5} Sammy Bedoui,⁶ Guillaume Lessene,^{1,5,7} Matthew E. Ritchie,^{3,5,8} David C.S. Huang,^{2,5} and Benjamin T. Kile^{1,5,*}

¹ACRF Chemical Biology Division

²Cancer and Haematology Division

³Molecular Medicine Division

⁴Molecular Genetics of Cancer Division

The Walter and Eliza Hall Institute of Medical Research, Parkville 3052, Australia

⁵Department of Medical Biology

⁶Department of Microbiology and Immunology

⁷Department of Pharmacology and Therapeutics

⁸Department of Mathematics and Statistics

The University of Melbourne, Parkville 3010, Australia

⁹Integrated Department of Immunology, University of Colorado Denver School of Medicine and National Jewish Health, Denver, CO 80206, USA

*Correspondence: mwhite@wehi.edu.au (M.J.W.), kile@wehi.edu.au (B.T.K.)

<http://dx.doi.org/10.1016/j.cell.2014.11.036>

SUMMARY

Activated caspases are a hallmark of apoptosis induced by the intrinsic pathway, but they are dispensable for cell death and the apoptotic clearance of cells *in vivo*. This has led to the suggestion that caspases are activated not just to kill but to prevent dying cells from triggering a host immune response. Here, we show that the caspase cascade suppresses type I interferon (IFN) production by cells undergoing Bak/Bax-mediated apoptosis. Bak and Bax trigger the release of mitochondrial DNA. This is recognized by the cGAS/STING-dependent DNA sensing pathway, which initiates IFN production. Activated caspases attenuate this response. Pharmacological caspase inhibition or genetic deletion of caspase-9, Apaf-1, or caspase-3/7 causes dying cells to secrete IFN- β . *In vivo*, this precipitates an elevation in IFN- β levels and consequent hematopoietic stem cell dysfunction, which is corrected by loss of Bak and Bax. Thus, the apoptotic caspase cascade functions to render mitochondrial apoptosis immunologically silent.

INTRODUCTION

Caspases are a family of 12 cysteinyl aspartate-specific proteases traditionally classified as inflammatory or apoptotic (McIlwain et al., 2013). Inflammatory caspases (caspase-1, -4, -5, and -12 in humans) mediate innate immune responses by cleaving precursors of proinflammatory cytokines such as IL-

1 β and IL-18, thereby facilitating their secretion. The apoptotic caspases (caspase-3, -6, -7, -8, and -9) play a role in the regulation of programmed cell death.

Apoptosis comprises two convergent pathways: the intrinsic and extrinsic (Youle and Strasser, 2008). The intrinsic pathway is controlled by the BCL-2 family of proteins, which is divided into three groups. The first contains prodeath BAK and BAX, the essential effectors of the pathway. Second are the pro-survival proteins (BCL-2, BCL-X_L, BCL-W, MCL-1, and A1), whose function is to prevent activation of BAK and BAX by physically restraining them and by sequestering a third group of BCL-2 family members, the prodeath “BH3-only” proteins (e.g., BIM and BID). In a healthy cell, prosurvival proteins keep BAK and BAX in check. Apoptotic signals trigger the BH3-only proteins to activate BAK/BAX. The latter induce mitochondrial outer-membrane permeabilization (MOMP), facilitating the efflux of factors, including cytochrome c, into the cytoplasm. Cytochrome c forms the apoptosome complex with APAF-1 and the inactive zymogen of the initiator caspase, caspase-9. This results in the activation of caspase-9, which then triggers the rest of the caspase cascade, culminating in activation of the effector caspases, caspase-3 and caspase-7.

The purpose of the caspase cascade remains an enigma. It mediates many of the hallmarks of apoptosis *in vitro*, such as DNA fragmentation and phosphatidylserine (PS) exposure, but is largely dispensable for the apoptotic death and clearance of cells *in vivo*. The hematopoietic system is a good example: *Bak*^{-/-} *Bax*^{-/-} mice exhibit a massive accumulation of mature blood cells, whereas mice with an *Apaf-1*^{-/-}, *Casp9*^{-/-}, or *Casp3*^{-/-} *Casp7*^{-/-} hematopoietic system show no significant perturbations in blood cell number (Lakhani et al., 2006; Lindsten et al., 2000; Marsden et al., 2002). This dichotomy can be

explained by the fact that the “point of no return” in apoptosis is BAK/BAX-mediated mitochondrial damage. Cells lacking BAK and BAX are resistant to a wide range of apoptotic stimuli; they do not exhibit cytochrome *c* release or caspase activation and are able to maintain clonogenicity (i.e., they can survive and generate viable progeny) (Lindsten et al., 2000; Wei et al., 2001). In contrast, Apaf-1- or caspase-deficient cells exhibit only short-term resistance to apoptotic stimuli and do not retain clonogenic potential (Ekert et al., 2004; Marsden et al., 2002; van Delft et al., 2010). Thus, although clearly capable of accelerating apoptosis, these and many other studies indicate that the apoptotic caspase cascade is not required for death to occur.

This raises important questions as to why caspase-deficient mice exhibit phenotypic abnormalities. For example, loss of Apaf-1, caspase-9, or caspase-3 results in lethality associated with large ectopic cell masses in the forebrain (Kuida et al., 1996, 1998; Yoshida et al., 1998), and the hematopoietic stem cell (HSC) compartment is expanded in the absence of caspase-3 (Janzen et al., 2008). Although this suggests an accumulation of cells otherwise destined to die, in both cases, the evidence points to a more complex mechanism. In the brain, controversy exists as to the extent of cell death in mice lacking the caspase cascade, and recent studies indicate that changes in morphogen gradients may underpin aberrant forebrain development (Honarpour et al., 2001; Nonomura et al., 2013; Oppenheim et al., 2001).

HSCs present a similar conundrum. HSC survival is governed by BCL-2 family proteins. Deletion of prosurvival Mcl-1 leads to their death, whereas overexpression of Bcl-2 increases their number (Domen et al., 2000; Opferman et al., 2005). This has led to a model whereby a proportion of HSCs undergo apoptosis during the normal course of hematopoiesis; hence, a reduction in apoptosis is proposed to lead to accumulation of HSCs in vivo (Orelia and Dzierzak, 2007). The expansion of HSCs observed in caspase-3-deficient mice would accord with this notion. Intriguingly, however, the evidence suggests that, rather than accumulating through failure to die, *Casp3*^{-/-} HSCs proliferate due to abnormalities in cytokine signaling (Janzen et al., 2008), suggesting potential non-cell death roles for the apoptotic caspase cascade. In fact, apoptotic caspases are increasingly implicated in other cellular processes such as differentiation (Yi and Yuan, 2009). In some cases, these roles are a byproduct of, or are associated with, apoptosis; in others, they appear to be “nonapoptotic” in nature.

Here, we show that the caspase cascade functions during apoptosis to prevent dying cells from producing type I interferon (IFN). Bak- and Bax-mediated mitochondrial damage triggers the release of mitochondrial DNA (mtDNA), which is recognized by the cGAS/STING-mediated cytosolic DNA sensing pathway. In the absence of the apoptotic caspases, this leads to the induction of IFN- β transcription and IFN- β secretion by the dying cell. Loss of the caspase cascade leads to elevated IFN- β levels in vivo. This feeds back to, and has a profound impact on, the HSC compartment, which is highly sensitive to the effects of type I IFN. Thus the apoptotic caspase cascade regulates the immunological impact an apoptotic cell has on the host by preventing dam-

age-associated molecular pattern (DAMP) signaling induced by mtDNA.

RESULTS

HSC Expansion and Dysfunction in the Absence of Caspase-9

To define the requirement for the intrinsic apoptosis pathway (Figure 1A) in HSC homeostasis, we generated mice lacking Bak and Bax or caspase-9. Because these animals die postnatally, we first profiled the HSC-containing lineage⁻ Sca1⁺ Kit⁺ (LSK) population in fetal livers at embryonic (E) day 13.5. Relative to wild-type (WT) counterparts, the proportion of LSKs in *Bak*^{-/-} *Bax*^{-/-} fetal livers was unchanged (Figures 1B and 1C). In contrast, LSKs were increased ~5-fold in *Casp9*^{-/-} fetal livers. To establish whether this was hematopoietic cell intrinsic, we transplanted fetal liver cells (FLCs) into lethally irradiated WT recipients. 12–16 weeks posttransplantation, a small but statistically significant increase in LSKs was observed in mice that received *Bak*^{-/-} *Bax*^{-/-} FLCs (Figures 1D and 1E). Recapitulating the situation in the fetal liver, the bone marrow of mice reconstituted with *Casp9*^{-/-} cells contained 5-fold more LSKs than those transplanted with WT cells. Collectively, these data suggested that HSC numbers are expanded in the absence of caspase-9. This was a counterintuitive result, given that Bak and Bax are the critical mediators of the intrinsic apoptosis pathway, whereas the downstream caspase cascade is thought to be dispensable for cell death.

To examine HSC function, WT, *Bak*^{-/-} *Bax*^{-/-}, or *Casp9*^{-/-} fetal liver test cells were mixed 50:50 with WT competitor cells and transplanted into lethally irradiated WT recipients (Figure 1F). 16 weeks posttransplant, the contribution of *Bak*^{-/-} *Bax*^{-/-} cells to peripheral blood B and T lymphocytes, myeloid cells, and bone marrow LSKs significantly outweighed that of WT competitor cells (Figures 1G and S1A available online). In contrast, *Casp9*^{-/-} peripheral blood B and T lymphocytes, myeloid cells, and bone marrow LSKs were present in equal numbers to WT competitors, suggesting that, despite the aberrant LSK profile, the *Casp9*^{-/-} fetal liver contains either (1) normal numbers of HSCs or (2) more HSCs than WT, but they are functionally impaired. We therefore tested the self-renewal capacity of HSCs by harvesting bone marrow from primary recipients and transplanting it into secondary recipients (Figures 1H, 1I, and S1B). In contrast to WT and *Bak*^{-/-} *Bax*^{-/-} cells, *Casp9*^{-/-} bone marrow exhibited a profoundly reduced contribution to peripheral blood B and T lymphocytes, myeloid cells, and bone marrow LSKs at 16 weeks post-secondary transplantation (Figure 1I), indicating that HSC function is severely compromised in the absence of caspase-9.

HSC Dysfunction in Caspase-9-Deficient Mice Is Cell Extrinsic

To establish whether LSK expansion in *Casp9*^{-/-} mice was intrinsic to the LSK population itself, we generated mixed bone marrow chimeras by transplanting WT or *Casp9*^{-/-} E13.5 FLCs with WT filler FLCs into lethally irradiated recipients. Consistent with our previous observations, 12–16 weeks later, we observed an expansion of *Casp9*^{-/-} LSKs in the WT:*Casp9*^{-/-} chimeras.

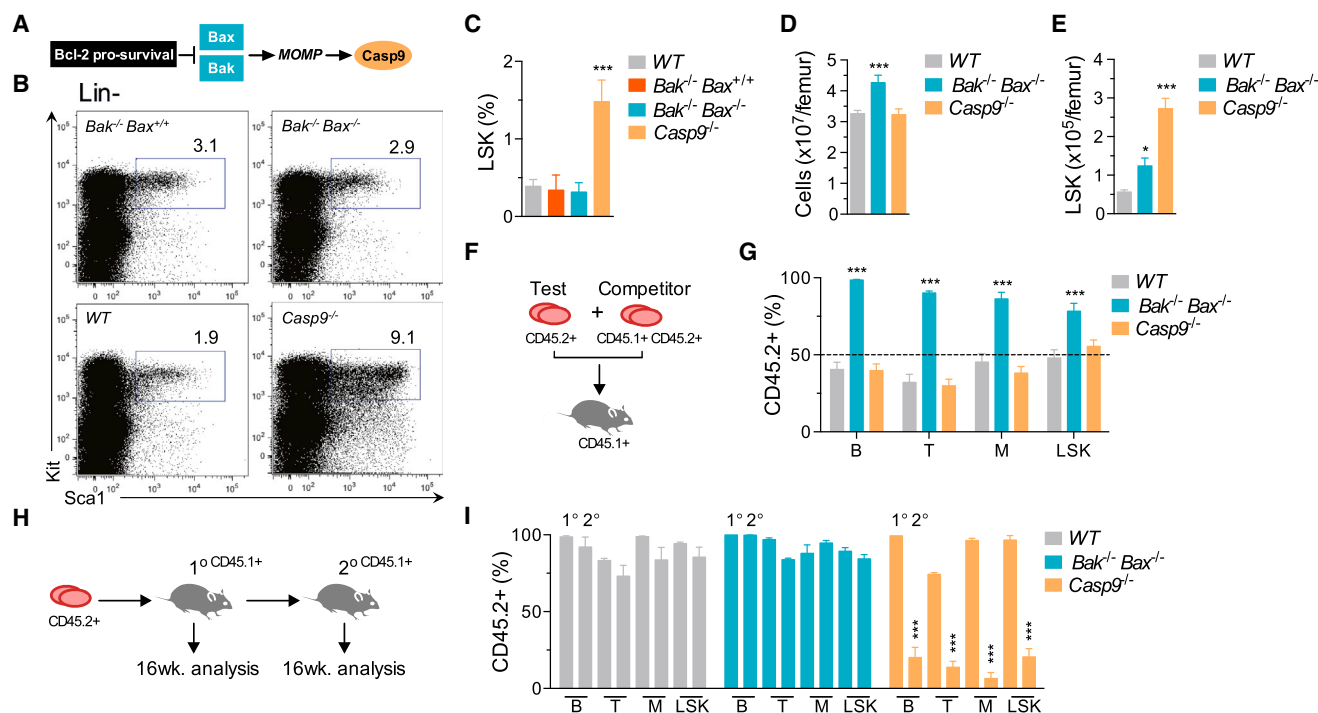


Figure 1. Deficiency of Caspase-9, but Not Bak and Bax, Impairs Hematopoietic Stem Cell Function

(A) The intrinsic apoptosis pathway.
 (B) Representative plots of LSK cell frequency in E13.5 fetal livers (gates display percentage of Lin⁻).
 (C) FACS analysis of LSKs in WT (n = 9), *Bak*^{-/-} *Bax*^{+/+} (n = 5), *Bak*^{-/-} *Bax*^{-/-} (n = 7), and *Casp9*^{-/-} (n = 10) E13.5 fetal livers.
 (D) Bone marrow cellularity in recipients of WT (n = 15), *Bak*^{-/-} *Bax*^{-/-} (n = 8), and *Casp9*^{-/-} (n = 9) FLCs 12–16 weeks posttransplant.
 (E) Donor-derived LSK cells in WT (n = 15), *Bak*^{-/-} *Bax*^{-/-} (n = 8), and *Casp9*^{-/-} (n = 9) bone marrow chimeras 12–16 weeks posttransplant.
 (F) Fetal liver competitive transplantation assay.
 (G) Proportion of CD45.2⁺ peripheral blood B lymphocytes, T lymphocytes, myeloid cells, and bone marrow LSK cells 16 weeks after competitive transplantation (n = 3–4 E13.5 test-CD45.2⁺ fetal livers per genotype and three recipients per donor mix). See also Figure S1.
 (H) Secondary transplantation assay.
 (I) Donor-CD45.2⁺ contribution to peripheral blood B lymphocyte, T lymphocyte and myeloid cells, and bone marrow LSK cells of 1° and 2° recipients 16 weeks posttransplant (n = 3–5 donor fetal livers per genotype and 2–3 recipients per donor bone marrow) See also Figure S1.
 Means were compared to WT using a one-way ANOVA with Bonferroni correction. Data represent the mean ± SEM. *p ≤ 0.05, **p ≤ 0.01, and ***p ≤ 0.005.

Strikingly, WT LSK numbers were also significantly increased relative to those in WT:WT chimeras (Figure 2A). Their Sca1 expression profile resembled that of *Casp9*^{-/-} Lin⁻ Kit⁺ cells (Figure 2B). Thus, WT LSKs expand in the presence of caspase-9-deficient hematopoietic cells, suggesting that HSC expansion in *Casp9*^{-/-} mice is driven by cell-extrinsic factors.

Caspase-9-Deficient HSPCs Exhibit a Type I Interferon Response Signature

We therefore analyzed the gene expression profile of Lineage⁻ Kit⁺ CD45.2⁺ hematopoietic stem and progenitor cells (HSPCs) harvested primary bone marrow chimeras. 495 genes (corresponding to 602 probes) were significantly upregulated in *Casp9*^{-/-} HSPCs (Figure 2C and Table S1 available online), with 275 genes (corresponding to 346 probes) differentially expressed (DE) in *Bak*^{-/-} *Bax*^{-/-} HSPCs. In *Casp9*^{-/-} HSPCs, gene set enrichment analysis using Camera identified enrichment for multiple type I IFN response signatures that were not apparent in *Bak*^{-/-} *Bax*^{-/-} HSPCs (Figures 2D and 2E). The top ten upregulated genes in *Casp9*^{-/-} HSPCs by fold change

were all type I IFN targets (Table S1). Quantitative PCR (qPCR) analysis of canonical type I IFN-stimulated genes (ISGs) confirmed their upregulation relative to WT in *Casp9*^{-/-} FLCs and bone marrow cells (Figures 2F and 2G). We therefore examined levels of the type I IFNs, IFN α and IFN β , in the serum of primary transplant recipients. Whereas IFN α was undetectable in all genotypic classes, we observed significantly elevated IFN β in mice reconstituted with *Casp9*^{-/-}, but not *Bak*^{-/-} *Bax*^{-/-}, cells (Figure 2H).

HSC Expansion in Caspase-9-Deficient Mice Is Caused by Type I Interferons

Type I IFNs have been shown to induce HSC proliferation, leading to functional exhaustion in vivo (Essers et al., 2009; Sato et al., 2009). We therefore generated mice doubly deficient for caspase-9 and the type I IFN receptor (Ifnar1). Although loss of Ifnar1 did not rescue postnatal lethality of *Casp9*^{-/-} mice (data not shown), deletion of Ifnar1 prevented LSK expansion in *Casp9*^{-/-} fetal livers (Figures 3A and 3B). Next, bone marrow chimeras were generated by reconstituting recipients

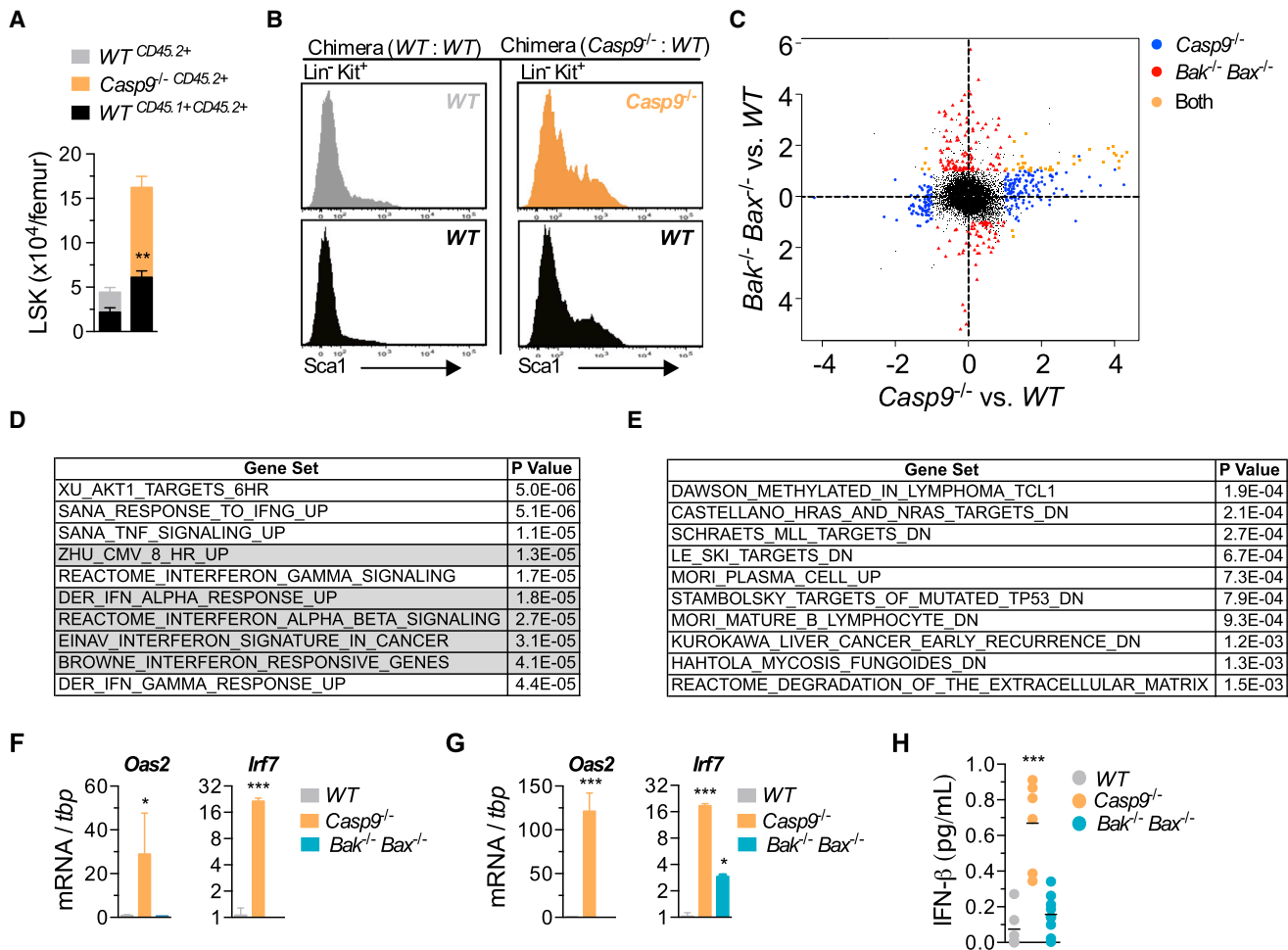


Figure 2. Loss of Caspase-9 Results in Elevated Type I Interferon In Vivo

(A) FACS analysis of mixed bone marrow chimeras 12–16 weeks posttransplant of WT (CD45.2⁺) or Casp9^{-/-} (CD45.2⁺) with WT “bystander” (CD45.1⁺CD45.2⁺) E13.5 FLCs into lethally irradiated CD45.1⁺ recipients. Number of donor-derived bone marrow LSK cells from both fractions is displayed (n = 8 mixed bone marrow chimeras per genotype from 3–4 fetal livers per genotype). Means of WT (CD45.1⁺CD45.2⁺) “bystander” cells were compared using a two-tailed t test. (B) Sca1 expression on Lin⁻Kit⁺ bone marrow cells from mixed bone marrow chimeras.

(C) Scatterplot of differentially expressed probes in microarray analysis of WT, Casp9^{-/-}, and Bak^{-/-} Bax^{-/-} Lin⁻Kit⁺CD45.2⁺ bone marrow cells. See also Table S1.

(D) Top ten gene sets (ranked by p value) from Gene Set Enrichment Analysis (GSEA) of Casp9^{-/-} in (C) (gray indicates type I IFN signatures).

(E) Top ten gene sets (ranked by p value) from GSEA of Bak^{-/-} Bax^{-/-} in (C).

(F and G) Real-time qPCR analysis of type I ISGs in fetal liver (F) and bone marrow cells (G) (n = 3–4 E13.5 fetal livers and 3–4 bone marrow chimeras per genotype).

(H) IFN-β protein in serum of WT (n = 6), Casp9^{-/-} (n = 6), and Bak^{-/-} Bax^{-/-} (n = 8) bone marrow chimeras.

Unless indicated, means were compared to WT using a one-way ANOVA with Bonferroni correction. Data represent the mean ± SEM. *p < 0.05, **p < 0.01, and ***p < 0.005.

with *Ifnar1*^{-/-} Casp9^{+/+}, *Ifnar1*^{+/+} Casp9^{-/-}, or *Ifnar1*^{-/-} Casp9^{-/-} FLCs. 16 weeks posttransplantation, recipients of *Ifnar1*^{+/+} Casp9^{-/-} cells exhibited a 5-fold increase in LSKs relative to mice that received *Ifnar1*^{-/-} Casp9^{+/+} cells (Figures 3C and 3D). In contrast, LSK numbers in *Ifnar1*^{-/-} Casp9^{-/-} chimeras were normal. Furthermore, deletion of *Ifnar1* restored the ability of Casp9^{-/-} HSCs to engraft the host and contribute to all major lineages upon secondary transplantation (Figures 3E and 3F). Collectively, our data indicate that loss of caspase-9 in vivo leads to production of IFN-β, which feeds back to the HSC compartment, resulting in loss of self-renewal capacity.

Apoptotic Mouse and Human Cells Produce Type I IFN When Caspases Are Inhibited

Activation of the apoptotic caspase cascade is impaired in the absence of caspase-9 (Li et al., 1997). We hypothesized that hematopoietic cells undergoing caspase-inhibited apoptosis might be the source of IFN-β. To test this, we treated WT murine splenocytes with the proapoptotic BH3 mimetic drug ABT-737, which targets the prosurvival proteins Bcl-x_L and Bcl-2 (Oltersdorf et al., 2005). ABT-737 induced caspase activation and cell death in splenocytes (Figures 4A and 4B). No IFN-β was detected in culture media of cells treated with ABT-737 alone. In

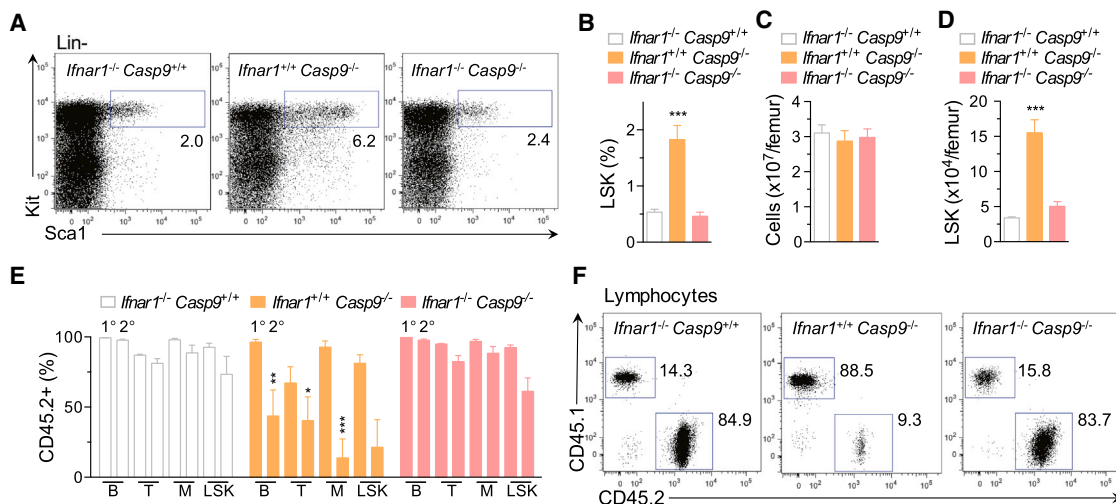


Figure 3. Type I Interferon Mediates the Hematopoietic Stem Cell Dysfunction Associated with Caspase-9 Loss

(A) Representative plots of LSK cell frequency in E13.5 fetal livers (gates display percentage of Lin⁻). (B) FACS analysis of LSKs in *Ifnar1*^{-/-} *Casp9*^{+/+} (n = 6), *Ifnar1*^{+/+} *Casp9*^{-/-} (n = 4), and *Ifnar1*^{-/-} *Casp9*^{-/-} (n = 6) E13.5 fetal liver. (C) Bone marrow cellularity from *Ifnar1*^{-/-} *Casp9*^{+/+} (n = 8), *Ifnar1*^{+/+} *Casp9*^{-/-} (n = 4), and *Ifnar1*^{-/-} *Casp9*^{-/-} (n = 5) bone marrow chimeras, 16 weeks posttransplant. (D) Number of donor-derived LSK cells from *Ifnar1*^{-/-} *Casp9*^{+/+} (n = 7), *Ifnar1*^{+/+} *Casp9*^{-/-} (n = 4), and *Ifnar1*^{-/-} *Casp9*^{-/-} (n = 5) bone marrow chimeras, 16 weeks posttransplant. (E) Donor-CD45.2⁺ contribution to the peripheral blood B lymphocyte, T lymphocyte, myeloid cells, and bone marrow LSK cells of 1[°] and 2[°] recipients at 16 weeks posttransplant. *Ifnar1*^{-/-} *Casp9*^{+/+} (n = 4), *Ifnar1*^{+/+} *Casp9*^{-/-} (n = 3), and *Ifnar1*^{-/-} *Casp9*^{-/-} (n = 4) donor fetal livers per genotype and three recipients per donor bone marrow. (F) Plots of representative analysis of donor contribution to 2[°] recipient lymphoid lineages in (E). Means were compared to WT using a one-way ANOVA with Bonferroni correction. Data represent the mean ± SEM. *p ≤ 0.05, **p ≤ 0.01, and ***p ≤ 0.005.

contrast, when apoptosis was triggered in the presence of the pan-caspase inhibitor Q-VD-Oph, IFN-β was produced (Figure 4C). To test whether this mechanism is conserved between mice and humans, peripheral blood mononuclear cells (PBMCs) were isolated from the blood of five healthy adult donors and treated with ABT-737. Caspase-3/7 activation and loss of cell viability was observed over 24 hr (Figures 4D and 4E). Upon co-incubation with ABT-737 and Q-VD-Oph, IFN-β secretion was observed in all five human PBMC samples (Figure 4F). These data demonstrated that, in both human and murine hematopoietic cells, caspase-inhibited apoptosis results in the production of IFN-β.

Apoptotic MEFs Produce Type I IFN When Caspases Are Inhibited

To better examine the role of the intrinsic apoptosis pathway, we utilized immortalized mouse embryonic fibroblasts (MEFs). WT MEFs are dependent on the prosurvival proteins Mcl-1 and Bcl-x_L for survival (Figure 5A). MEFs lacking Mcl-1 undergo Bak- and Bax-mediated apoptosis in response to ABT-737 (van Delft et al., 2006). We therefore treated multiple *Mcl1*^{-/-} MEF lines with increasing concentrations of ABT-737 and co-incubated them with either Q-VD-Oph or another pancaspase inhibitor, z-VAD.fmk. ABT-737 treatment of *Mcl1*^{-/-} MEFs induced caspase-3/7 activity and cell death (Figures 5B and 5C). Coincubation with either z-VAD.fmk or Q-VD-Oph blocked caspase activation and prevented loss of viability. Although undetectable in supernatant from *Mcl1*^{-/-} MEFs treated with

ABT-737 or caspase inhibitor alone, IFN-β was induced when ABT-737 (or other apoptotic stimuli) (Figure S2) was combined with z-VAD.fmk or Q-VD-Oph (Figure 5D). Upregulation of *Ifnb1*, the gene encoding IFN-β, was evident 4 hr posttreatment (Figure 5E). These data demonstrate that nonhematopoietic cells also produce IFN-β when undergoing caspase-inhibited apoptosis and implicate Bak and Bax as the initiators of the signal that triggers IFN-β production.

The Apoptotic Caspase Cascade Suppresses Bak/Bax-Mediated Type I IFN Production

To confirm whether Bak and Bax activation induces IFN-β production, we triggered mitochondrial apoptosis in WT, *Casp9*^{-/-}, and *Bak*^{-/-} *Bax*^{-/-} *Casp9*^{-/-} MEF lines by combining ABT-737 treatment with expression of Bim_{S2A}, which targets Mcl-1 (Lee et al., 2008). Expression of Bim_{S4E}, an inert form of Bim, served as a negative control. *Casp3*^{-/-} *Casp7*^{-/-} MEF lines were included to determine whether deletion of the effector caspases causes IFN production. In WT cells expressing Bim_{S2A}, ABT-737 treatment induced a 3-fold increase in caspase activity and an ~75% loss of viability (Figures 5F–5H). In contrast, both *Casp9*^{-/-} and *Bak*^{-/-} *Bax*^{-/-} *Casp9*^{-/-} cells were resistant to Bim_{S2A} + ABT-737. Analysis of the supernatant demonstrated abundant IFN-β secretion by *Casp9*^{-/-} and *Casp3*^{-/-} *Casp7*^{-/-} cells treated with Bim_{S2A} + ABT-737, but not WT or *Bak*^{-/-} *Bax*^{-/-} *Casp9*^{-/-} counterparts (Figures 5I and S3). These data demonstrated that, in vitro, induction of Bak- and Bax-mediated apoptosis stimulates type I IFN

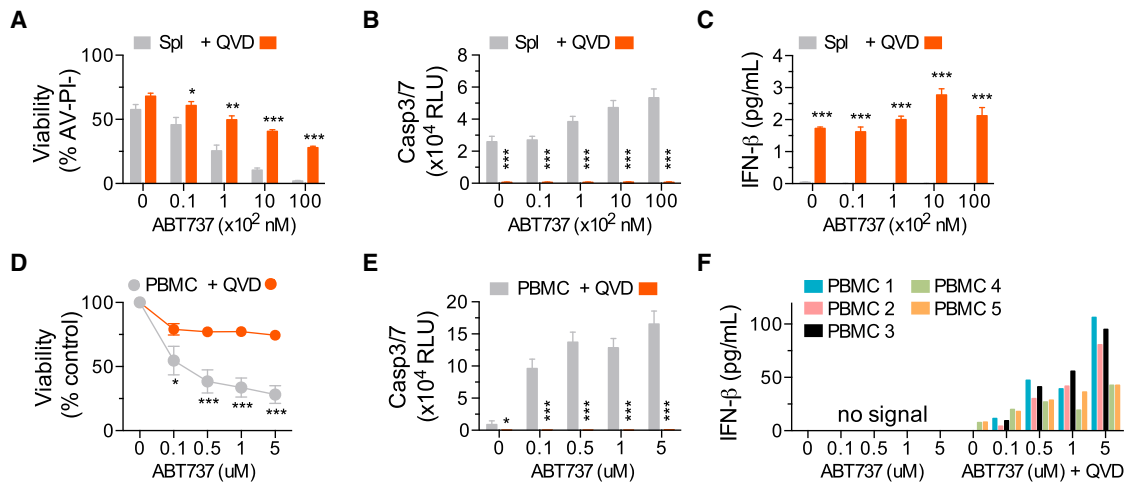


Figure 4. Apoptotic Hematopoietic Cells Produce Type I Interferon When Caspases Are Inhibited

(A) Viability of murine splenocytes treated with ABT-737 ± 20–30 μM Q-VD-OPh (QVD) for 24 hr.

(B and C) (B) Caspase activity and (C) IFN-β in culture supernatant after 24 hr of treatment (n = 4 mice). Means were compared using a two-tailed t test. Data represent the mean ± SEM. *p ≤ 0.05, **p ≤ 0.01, and ***p ≤ 0.005.

(D) Percentage of viable human PBMCs as quantitated by ATP levels (CellTiterGlo) after 24 hr of treatment with ABT-737 and coincubation with 20–30 μM Q-VD-OPh (QVD).

(E) Bar graphs of caspase activity after 6 hr and (F) IFN-β in culture supernatant after 24 hr (n = 5 healthy donor blood samples). Representative of two independent experiments.

production when either the apoptotic initiator (caspase-9) or effector (caspase-3/7) caspases are inactivated.

We reasoned that eliminating Bak and Bax would remove the stimulus for IFN-β production in caspase-deficient mice. To test this, we generated *Casp9*^{-/-}, *Apaf1*^{-/-}, *Casp3*^{-/-}, *Casp3*^{-/-} *Casp7*^{-/-}, and *Bak*^{-/-} *Bax*^{-/-} *Casp9*^{-/-} bone marrow chimeras. 16 weeks posttransplantation, LSKs were increased in recipients of *Apaf1*^{-/-}, *Casp9*^{-/-} or *Casp3*^{-/-} *Casp7*^{-/-} cells, demonstrating that inhibition of the apoptotic caspase cascade at either the apoptosome or effector stage triggers LSK expansion (Figures 5J and 5K). In contrast, the LSK profile in *Bak*^{-/-} *Bax*^{-/-} *Casp9*^{-/-} chimeras was unchanged. Thus, in the absence of Bak- and Bax-mediated apoptosis, deletion of caspases does not cause LSK expansion. Accordingly, IFN-β levels in *Bak*^{-/-} *Bax*^{-/-} *Casp9*^{-/-} chimeras were equivalent to WT, and no upregulation of type I IFN response genes was apparent (Figures 5L and 5M). Secondary bone marrow transplants confirmed that loss of Bak/Bax-mediated apoptosis also rescued HSC function, with *Bak*^{-/-} *Bax*^{-/-} *Casp9*^{-/-} bone marrow efficiently engrafting the host and contributing to the LSK compartment and all major lineages (Figure 5N). Thus, deletion of Bak and Bax prevents IFN-β production and HSC dysfunction in mice lacking a functional apoptotic caspase cascade.

Dying Cells Upregulate Type I IFN Production in a Cell-Intrinsic Manner

We next examined whether apoptotic cells secrete IFN-β in a cell-intrinsic manner. *Ifnar1*^{-/-} *Casp9*^{-/-} MEFs were transduced with Bim_S2A-GFP or Bim_S4E-GFP and co-plated with unmanipulated *Ifnar1*^{-/-} MEFs (Figures 6A and 6B). *Ifnar1*-deficient cells were utilized to eliminate paracrine/autocrine effects of IFN-β. Cocultures were treated with ABT-737, which induced

apoptosis in the *Ifnar1*^{-/-} *Casp9*^{-/-} Bim_S2A-GFP cells, but not the other three cell populations. Subsequently, GFP⁺ (apoptotic or nonapoptotic) and GFP⁻ (bystander) cells were sorted, and expression of *Ifnb1* was analyzed by qPCR. Relative to healthy bystanders, a significant upregulation of *Ifnb1* mRNA was observed in apoptotic, but not nonapoptotic, cells (Figures 6B and 6C). When using WT (rather than *Ifnar1*^{-/-}) bystanders, type I IFN response genes were strongly induced in bystanders cocultured with apoptotic cells (Figure 6D), indicating that cells undergoing caspase-inhibited apoptosis actively transcribe *Ifnb1* and secrete bioactive IFN-β.

Apoptotic IFN Production Is Driven by Mitochondrial DNA

Considering the mechanism by which Bax and Bax stimulate a cell to produce type I IFN, we reasoned that release of a mitochondrial factor into the cytoplasm could be the initiating event. In the context of microbial invasion, type I IFNs are induced by a range of pathogen-associated molecular patterns (PAMPs). Viral nucleic acids are an important, and potent, example. Their presence is detected by cytosolic receptors that activate signaling cascades leading to the upregulation of IFN transcription (Paludan and Bowie, 2013). We hypothesized that Bak- and Bax-mediated damage to mitochondria may cause the release of mtDNA and that the latter would act as a DAMP capable of recognition by the dying cell's innate nucleic acid sensors. We therefore generated mtDNA-depleted cells (so-called “ρ⁰” cells) by culturing *Mcl1*^{-/-} MEFs in ethidium bromide (King and Attardi, 1989). qPCR analysis revealed a near-complete absence of mtDNA after three passages (Figures 6E and S4). Expression profiling of ρ⁰ cells demonstrated that 28 genes (corresponding to 42 probes)

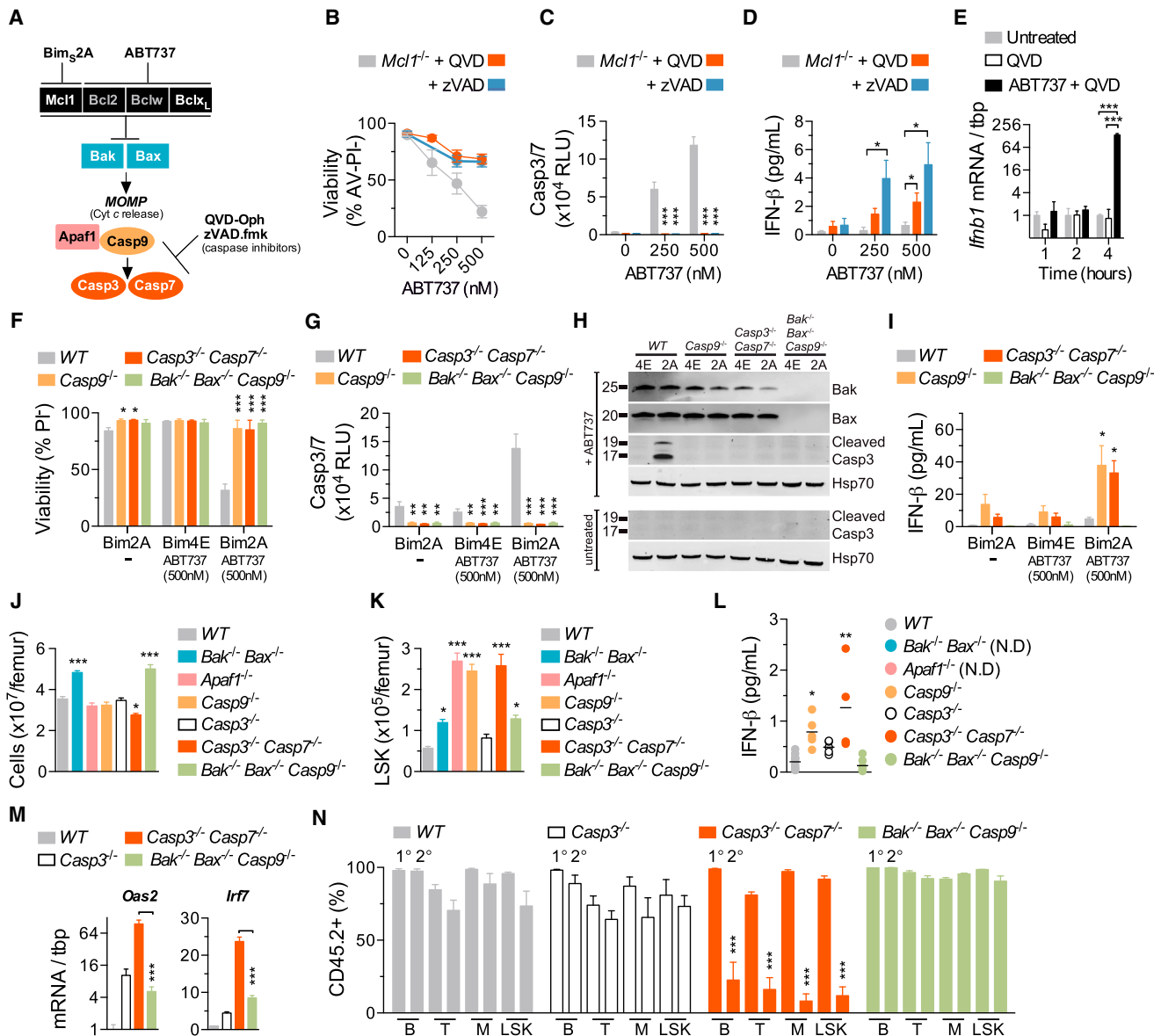


Figure 5. Disabling Caspases Downstream of Bak and Bax Triggers Type I IFN Production

(A) Schematic diagram of the manipulation of intrinsic apoptosis in MEFs.

(B–D) (B) Viability of MEFs treated with ABT-737 ± 20–30 μM of Q-VD-Oph (QVD) or z-VAD.fmk (zVAD) for 24 hr, (C) bar graphs of caspase activity after 6 hr, and (D) IFN-β in supernatant after 24 hr (n = 9 independent MEF lines). Means were compared using a two-tailed t test. See also Figure S2.

(E) Real-time qPCR analysis of *Ifnb1* induction in *Mcl1*^{-/-} MEFs (n = 3 independent MEF lines). Means were compared using a two-tailed t test.

(F and G) (F) Viability of MEFs expressing Bim_s2A or Bim_s4E and treated with ABT-737 for 20–24 hr and (G) caspase activity after 6 hr.

(H and I) (H) Immunoblot of lysates of MEFs treated with ABT-737 (1 μM) for 4 hr and (I) bar graph of IFN-β in supernatant after 20–24 hr (n = 3 independent MEF lines per genotype). See also Figures S2 and S3.

(J) Bone marrow cellularity from WT (n = 22), *Bak*^{-/-} *Bax*^{-/-} (n = 8), *Apaf1*^{-/-} (n = 5), *Casp9*^{-/-} (n = 11), *Casp3*^{-/-} (n = 13), *Casp3*^{-/-} *Casp7*^{-/-} (n = 7), and *Bak*^{-/-} *Bax*^{-/-} *Casp9*^{-/-} (n = 9) bone marrow chimeras.

(K) Number of donor-derived LSK cells from WT (n = 22), *Bak*^{-/-} *Bax*^{-/-} (n = 8), *Apaf1*^{-/-} (n = 5), *Casp9*^{-/-} (n = 11), *Casp3*^{-/-} (n = 13), *Casp3*^{-/-} *Casp7*^{-/-} (n = 7), and *Bak*^{-/-} *Bax*^{-/-} *Casp9*^{-/-} (n = 9) bone marrow chimeras.

(L) IFN-β in serum of WT (n = 10), *Casp9*^{-/-} (n = 5), *Casp3*^{-/-} (n = 5), *Casp3*^{-/-} *Casp7*^{-/-} (n = 4), and *Bak*^{-/-} *Bax*^{-/-} *Casp9*^{-/-} (n = 7) bone marrow chimeras. Not done, N.D.

(M) Real-time qPCR analysis of type I ISGs in bone marrow cells (n = 3–4 bone marrow chimeras per genotype). Means were compared using a two-tailed t test. (N) Donor-CD45.2⁺ contribution to the peripheral blood B lymphocyte, T lymphocyte, myeloid cells, and bone marrow LSK cells of 1° and 2° recipients 16 weeks posttransplant (n = 3 donor fetal livers per genotype and 3 recipients per donor bone marrow).

Unless otherwise indicated, means were compared to WT using a one-way ANOVA with Bonferroni correction. Data represent the mean ± SEM. *p ≤ 0.05, **p ≤ 0.01, and ***p ≤ 0.005.

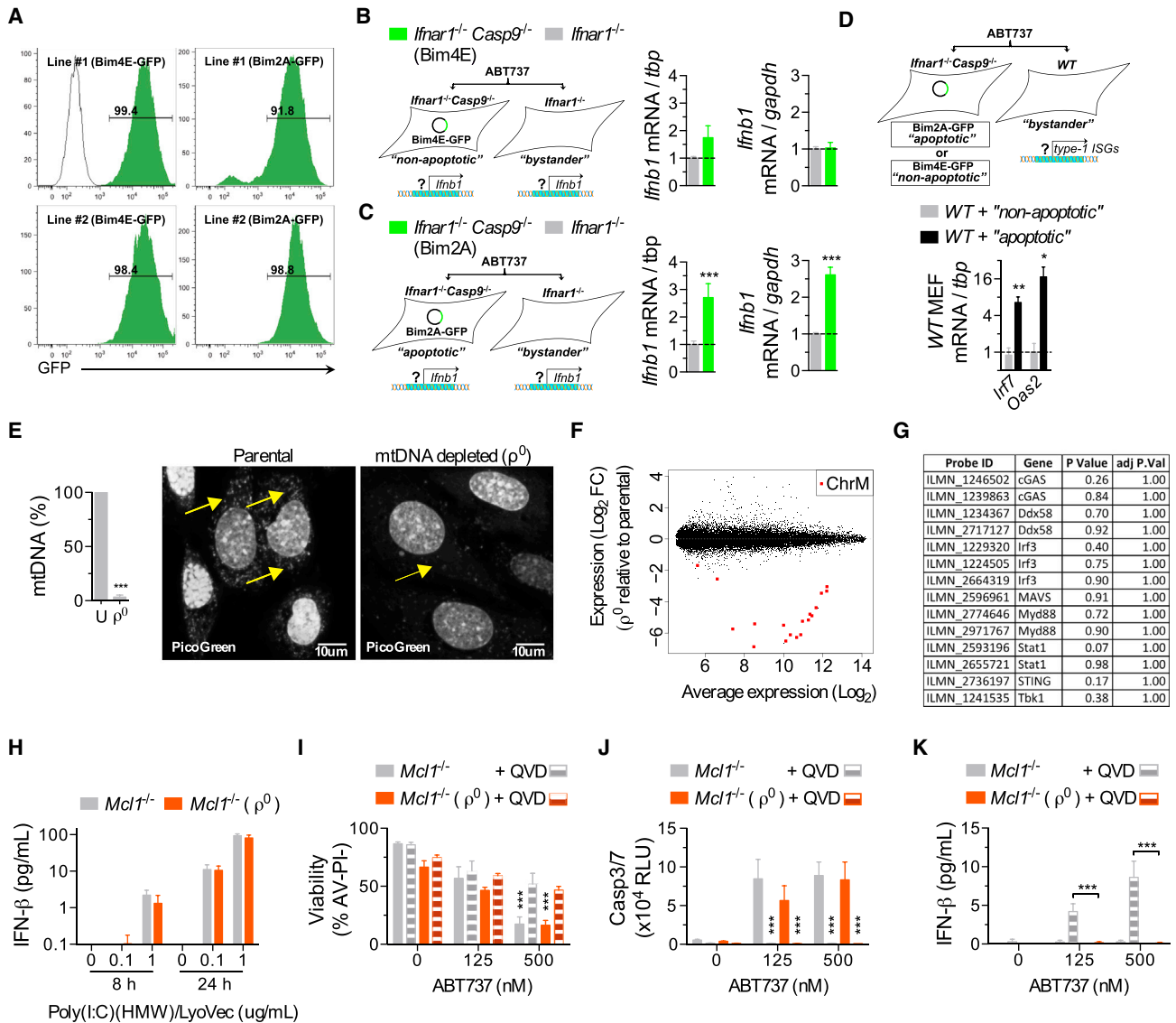


Figure 6. mtDNA Triggers Type I IFN Production during Caspase-Inhibited Apoptosis

(A) Representative plots of infection efficiency of the MEFs used in (B–D).
 (B and C) Real-time qPCR analysis of nonapoptotic (expressing Bim₄E, B) and apoptotic (expressing Bim₂A, C) MEFs and their respective *Ifnar1*^{-/-} bystander from cocultures after treatment with ABT-737 (500 nM) for 18–20 hr (data combined from three experiments, with two independent MEF lines per genotype). mRNA expression is shown relative to two independent housekeeping genes, *tbp* and *gapdh*.
 (D) Real-time qPCR analysis of WT bystanders from cocultures after treatment with ABT-737 for 18–20 hr (data combined from two experiments, with two independent MEF lines/genotype).
 (E) Real-time qPCR analysis of mtDNA content from *Mcl1*^{-/-} MEFs cultured in ethidium bromide to generate mtDNA-depleted (ρ^0) MEFs (used in F–J). Representative image of MEFs stained with PicoGreen nucleic acid stain. Arrows indicate mtDNA. Scale bars, 10 μ m. See also Figure S4.
 (F) Scatterplot of differentially expressed probes from microarray analysis of *Mcl1*^{-/-} ρ^0 MEFs compared to their respective parental *Mcl1*^{-/-} MEF. (n = 3 independent MEF lines). Chromosome M, ChrM. See also Table S2.
 (G) Table of a selected set of type I IFN response genes from analysis in (F).
 (H) Bar graph of IFN- β in the supernatant of ρ^0 and parental MEFs transfected with Poly(I:C)(HMW) (n = 3 independent MEF lines).
 (I–K) (I) Bar graphs of the viability of ρ^0 and parental MEFs treated with ABT-737 \pm 20–30 μ M of Q-VD-Oph (QVD) for 24 hr, (J) caspase activity after 6 hr, and (K) IFN- β in supernatant after 24 hr (n = 4 independent MEF lines).
 Means were compared using a two-tailed t test. Data represent the mean \pm SEM. *p \leq 0.05, **p \leq 0.01, and ***p \leq 0.005.

were downregulated and 61 genes (corresponding to 82 probes) were upregulated (Figure 6F and Table S2). 18 probes corresponding to 9 mitochondrially encoded genes were pre-

sent on the array. These were the most downregulated genes in ρ^0 cells (Camera p value = 0.0095). Gene set analysis using Camera detected no significant enrichment for any of the c2

expression signatures (data not shown). In addition, a subset of known type I IFN response genes was not significantly downregulated in ρ^0 cells (Figure 6G, Camera p value for downregulation = 0.45). Consistent with there being no functional impairment of IFN response pathways, ρ^0 cells responded normally when transfected with poly(I:C) (Figure 6H). Treatment of *Mcl1*^{-/-} ρ^0 cells with ABT-737 resulted in caspase activation and a loss of viability similar in magnitude to that exhibited by the parental lines (Figures 6I and 6J). In the presence of Q-VD-Oph, IFN- β production was observed in the parental, but not ρ^0 , cells (Figure 6K). These data indicate that mtDNA is the trigger for IFN production downstream of Bak- and Bax-mediated mitochondrial damage.

Bak/Bax-Mediated mtDNA Release Triggers cGAS/STING-Dependent IFN Production

Two major pathways that mediate type I IFN production in response to intracellular microbial DNA have been described (Paludan and Bowie, 2013). The first is initiated by Toll-like receptor 9 (Tlr9) recognition of DNA localized to endosomes, which triggers Myd88 signaling. Deletion of Myd88 in *Casp9*^{-/-} chimeras failed to normalize serum IFN- β levels and did not prevent LSK expansion (Figure S5), suggesting that mtDNA-induced IFN- β production does not require the Tlr-mediated endosomal recognition pathway. The second is the stimulator of interferon genes (STING) pathway (Barber, 2014). It is triggered when DNA binds to cyclic GMP-AMP synthase (cGAS), thereby catalyzing production of cyclic GMP-AMP dinucleotide (cGAMP), which binds to and activates STING. Activated STING induces type I IFN transcription via the Tbk1-Irf3 signaling axis. We treated splenocytes from WT and STING-deficient mice with ABT-737 in the presence or absence of Q-VD-Oph. ABT-737 induced apoptotic caspase activation and cell death in WT and *STING*^{-/-} cells with similar kinetics (Figures 7A and 7B). Coincubation with Q-VD-Oph triggered IFN- β secretion by WT, but not *STING*^{-/-}, cells (Figure 7C).

To further dissect the requirement for the STING pathway, we derived MEFs from *STING*^{-/-} mice and generated MEF lines lacking cGAS and Irf3 by CRISPR/Cas9-mediated gene targeting. All lines underwent apoptosis in response to ABT-737 and Bim_{S2A} (Figures 7D and 7E). WT cells produced IFN- β when coincubated with Q-VD-Oph. In contrast, *cGAS*^{CRISPR-/-}, *STING*^{-/-}, and *Irf3*^{CRISPR-/-} cells did not (Figure 7F). The requirement for Tbk1 was examined by pretreating *Mcl1*-deficient MEFs with the Tbk1 inhibitor MRT-67307. *Mcl1*^{-/-} cells undergoing caspase-inhibited apoptosis secreted IFN- β (Figures 7G and 7H). Addition of MRT-67307 suppressed IFN- β production by dying cells (Figure 7I). These data demonstrate that caspase-inhibited apoptosis triggers cGAS/STING/Tbk1/Irf3-mediated IFN- β production.

Recent evidence indicates that cGAS is activated via a direct interaction with cytosolic DNA (Civril et al., 2013; Sun et al., 2013). To establish whether mtDNA interacts with cGAS during caspase-inhibited apoptosis, we immunoprecipitated cGAS from *Mcl1*^{-/-} MEFs treated with ABT-737 and Q-VD-Oph and utilized qPCR analysis to detect coprecipitated DNA. Although there was no mtDNA enrichment when cGAS was immunoprecipitated from untreated cells, a significant enrichment for

mtDNA, but not genomic DNA, was observed in cells treated with ABT-737 and Q-VD-Oph (Figure 7J). Collectively, these data indicate that mtDNA is released, binds to, and activates cGAS during caspase-inhibited apoptosis.

DISCUSSION

Role of the Intrinsic Apoptosis Pathway in HSC Homeostasis

Deletion of Bak and Bax had no impact on the number of immunophenotypic HSCs in the fetal liver, suggesting that the intrinsic apoptosis pathway is dispensable for HSC homeostasis during development. Upon transplantation, recipients of *Bak*^{-/-} *Bax*^{-/-} FLCs exhibited a statistically significant 2-fold increase in bone marrow LSK number. This increase is similar to that reported for mice overexpressing Bcl-2 (Domen et al., 2000) and supports a role for the intrinsic pathway in regulating adult HSC homeostasis. However, a simpler explanation might be that HSCs lacking Bak and Bax are more resistant to the stresses of transplantation. Consistent with this, *Bak*^{-/-} *Bax*^{-/-} FLCs outcompeted WT counterparts in mixed transplants. Similar effects have been reported for HSCs lacking Bim (Labi et al., 2013). Thus, the extent to which death via the intrinsic apoptosis pathway shapes the HSC pool at steady state remains to be determined. It may be that programmed cell death does not represent a significant fate for HSCs. Alternatively, other cell death modalities such as the extrinsic apoptosis pathway or necroptosis might contribute to HSC homeostasis.

Apoptotic versus Nonapoptotic Roles for Apoptotic Caspases

Apoptotic caspases have been ascribed a number of functions beyond the internal demolition of dying cells. Some of these (e.g., prostaglandin-induced tumor cell repopulation [Huang et al., 2011] and AMPA receptor internalization [Li et al., 2010b]) appear to be a byproduct of apoptotic cell death. Others (e.g., iPS cell reprogramming [Li et al., 2010a] and microglia activation [Burguillos et al., 2011]) are thought to represent “nonapoptotic” roles for caspases. Our genetic experiments, both in vitro and in vivo, demonstrate that, in suppressing IFN production, the apoptotic caspases play an apoptotic role, i.e., function downstream of Bak and Bax. Unless Bak and Bax are activated, mtDNA is not released, and caspases are not required to attenuate mtDNA-induced DAMP signaling. This has two important implications. First, blocking the apoptotic caspase cascade during apoptosis triggers the production of IFN- β , a potentially significant confounding experimental factor. This should be considered whenever the apoptotic caspase cascade is genetically or pharmacologically manipulated. Perturbations in type I IFN signaling may explain some of the published biological roles for caspases. Second, the fact that caspase-deficient mice present with a dramatic increase in LSKs, whereas *Bak*^{-/-} *Bax*^{-/-} animals do not, initially suggested that caspases play a “nonapoptotic” role in HSCs. However, the subsequent experiments with *Bak*^{-/-} *Bax*^{-/-} *Casp9*^{-/-} cells and bone marrow chimeras demonstrated that the phenotype is dependent on Bak/Bax activation. This highlights the importance of establishing whether apoptotic caspase activation in a given setting is the result of

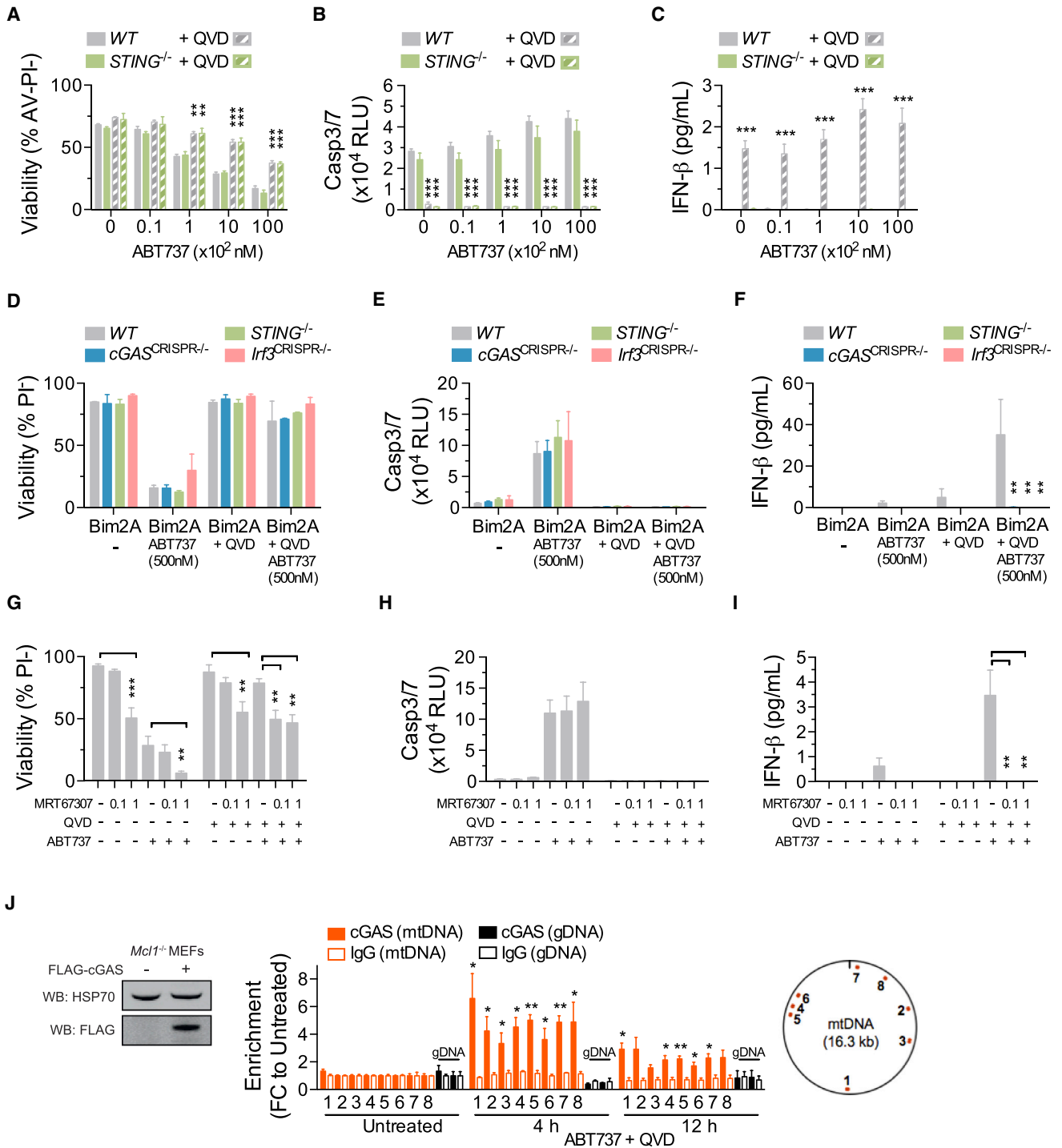


Figure 7. mtDNA Release into the Cytosol Triggers cGAS-STING-Tbk1-Irf3-Mediated Type I Interferon Production
 (A–C) (A) Viability of murine splenocytes treated with ABT-737 ± 20–30 μM Q-VD-OPH (QVD) for 24 hr, (B) caspase activity after 6 hr, and (C) IFN-β in culture supernatant after 24 hr (n = 4 mice per genotype). Means were compared to WT using a one-way ANOVA with Bonferroni correction.
 (D–F) (D) Viability of MEFs treated with ABT-737 ± 20–30 μM Q-VD-OPH (QVD) for 24 hr, (E) caspase activity after 6 hr, and (F) IFN-β in culture supernatant after 24 hr (n = 3 independent MEF lines per genotype, or 3 independent CRISPR/Cas9-targeted MEF clones). Means were compared to WT using a one-way ANOVA with Bonferroni correction.
 (G–I) (G) Bar graphs of the viability of *Mcl1*^{-/-} MEFs pretreated for 1 hr with MRT-67307 (μM) followed by ABT-737 (500 nM) ± 20–30 μM Q-VD-OPH (QVD) for 24 hr, (H) caspase activity after 6 hr, and (I) IFN-β in culture supernatant after 24 hr (n = 3 independent MEF lines).

(legend continued on next page)

upstream mitochondrial damage or an alternative signaling mechanism.

mtDNA Activates the STING-Dependent Cytosolic DNA Sensing Pathway

Our data indicate that Bak/Bax-dependent mtDNA release triggers the cGAS/STING-dependent cytosolic DNA sensing pathway. mtDNA released during cell death has been previously reported to provide a second signal that cooperates with signal 1 (e.g., LPS) to activate the NLRP3 inflammasome and induce IL-1 β production (Shimada et al., 2012). Whether mtDNA released via Bak/Bax also activates the inflammasome is unclear. However, other than IFN- β , mice with a caspase-9-deficient hematopoietic system did not exhibit elevated proinflammatory cytokine serum levels or any signs of systemic autoinflammatory disease when aged to 12 months (Figure S6). This suggests that, at least in the context of steady-state hematopoietic cell turnover, Bak/Bax-mediated mtDNA release does not result in unbridled inflammasome activity when the caspase cascade is inactivated. Whether the elevations in IFN- β caused by loss of the caspase cascade lead to the development of autoimmune disease over the longer term and whether perturbations in caspase activity might contribute to human autoinflammatory/autoimmune disease remain to be established.

Mechanisms of Caspase-Mediated Suppression of Type I IFN

During apoptosis, caspases orchestrate a global program of cellular demolition, targeting ~1,000 protein substrates (Crawford and Wells, 2011). They cause DNA damage, suppress transcription, shut down protein translation, and disable a host of other essential cellular processes. Unlike genomic damage, which is triggered by cleavage of iCAD, the inhibitor of caspase-activated DNase (CAD) (Enari et al., 1998), and PS exposure, which is facilitated by cleavage of Xkr8 (Suzuki et al., 2013), it seems likely that caspase-mediated suppression of IFN- β production (and DAMP signaling generally) is the result of multiple redundant processes. First, the fact that apoptotic CAD^{CRISPR-/-} MEFs secrete detectable amounts of IFN- β suggests that CAD-mediated genomic damage contributes to the attenuation of gene expression (Figure S7). Second, caspase-3/7 might cleave and inactivate a component or components of the type I IFN production pathway. There is evidence that IFN signaling intermediates, including Irf3, can be targeted by caspases (Crawford et al., 2013). Third, caspase-3/7 could mediate the degradation of mtDNA, thereby preventing its interaction with cGAS. This might occur via CAD or perhaps lysosomal deoxyribonuclease (DNase) II, which can digest the genomic DNA of engulfed cells. Although the precise contribution these and other mechanisms make to suppressing IFN- β

production in apoptotic cells remains to be established, it seems unlikely that any one of them is solely responsible. We suggest that caspase-mediated acceleration of cell death and suppression of DAMP signaling are inextricably linked. Both outcomes are achieved via global cellular demolition.

Potential Crosstalk between Apoptosis and Necroptosis

Necroptosis is a regulated form of necrotic cell death mediated by receptor-interacting protein kinase 3 (RIPK3) and the pseudokinase M1K1 (Linkermann and Green, 2014). It is triggered by prodeath ligands like TNF α and requires the inhibition or loss of caspase-8. In vitro, necroptosis is typically induced by TNF α and a caspase inhibitor such as z-VAD.fmk or Q-VD-Oph. The latter are both broad-spectrum inhibitors that target caspase-8, caspase-9, and caspase-3/7 (Chauvier et al., 2007). If necroptotic stimuli induce mitochondrial damage and mtDNA release, our results would predict that pan-caspase inhibition would result in IFN production by dying cells. Previous studies suggest that necroptosis triggered by TNF α , z-VAD.fmk, and cycloheximide causes Bak/Bax-dependent mitochondrial damage (Irrinki et al., 2011) and that Bak^{-/-} Bax^{-/-} MEFs are partially protected from necroptotic death induced by TNF α , Q-VD-Oph, and a Smac mimetic (TSQ) (Moujalled et al., 2013). Given that, like TNF α , type I IFNs, in combination with caspase inhibition, can induce necroptosis (Dillon et al., 2014; Thapa et al., 2013), our data suggest the potential for feed-forward effects driven by mtDNA-induced IFN production during caspase-inhibited necroptosis.

Pharmacological Inhibition of Apoptotic Caspases

Several caspase inhibitors have undergone clinical trials. They include the caspase-1 inhibitors VX-740 and VX-765 (Belnacasan) and the pan-caspase inhibitors IDN-6556 (Emricasan) and GS-9450 (O'Brien and Dixit, 2009). To date, none have received approval, although IDN-6556 is in ongoing trials for a number of indications, including alcoholic hepatitis, hepatic impairment, and islet transplantation. Evidence that VX-765 can block the pyroptotic death of HIV-infected CD4 T cells (Doitsh et al., 2014) has added to the hope that caspase inhibitors may yet find clinical application. That study highlighted their potential as a new class of antiviral drugs that target the host, not the virus. Our findings support this notion from an entirely different angle, suggesting that apoptotic caspase inhibition might be an effective means of amplifying endogenous IFN production. It will be interesting to see whether patients treated with a pancaspase inhibitor exhibit elevations in IFN- β levels.

Caspases Negatively Regulate DAMP Signaling

The traditional classification of caspases as inflammatory or apoptotic has broken down in the last decade, as it has become

(J) Immunoprecipitation (IP) followed by PCR. Left, immunoblot of lysates taken from Mcl1^{-/-} MEFs transduced with an expression plasmid encoding FLAG-cGAS. Right, data represent the fold change (FC) in enrichment of DNA fragments using anti-FLAG or IgG (negative control) to coprecipitate DNA in untreated MEFs or MEFs treated with ABT-737 (1 μ M) and Q-VD-Oph (QVD) (30 μ M) for the indicated time. DNA fragments were amplified by real-time qPCR using eight primer pairs for mtDNA and two primer pairs for gDNA. The relative locations of the mtDNA amplicons are shown (data are combined from two, with three replicates). Means were compared between treated and untreated samples.

See also Figures S5, S6, and S7.

Unless otherwise stated, means were compared using a two-tailed t test. Data represent the mean \pm SEM. *p \leq 0.05, **p \leq 0.01, and ***p \leq 0.005.

apparent that inflammatory caspases such as caspase-1 can kill and that apoptotic caspases can mediate non-death processes. Our findings demonstrate that caspase-9, -3, and -7 are essential negative regulators of mtDNA-induced DAMP signaling. Although apoptotic caspases have been previously reported to inactivate the DAMPs HMGB1 (Kazama et al., 2008) and IL-33 (Cayrol and Girard, 2009; Lüthi et al., 2009), the absence of autoinflammatory disease in caspase-9-deficient bone marrow chimeras suggests that, at least in the context of the hematopoietic system, apoptotic caspases are dispensable for their regulation. Alternatively, IFN- β may mask their effects. A very cogent review of this subject recently proposed that mammalian caspases “can be construed to act as either positive or negative regulators of inflammation” (Martin et al., 2012). Given that type I IFNs are pleiotropic in nature, possessing both inflammatory and anti-inflammatory properties (Prinz and Knobloch, 2012), our results indicate that the apoptotic caspases serve as both.

EXPERIMENTAL PROCEDURES

Experimental Animals

All mice were backcrossed for at least ten generations on a C57BL/6 background. *Apaf1*^{-/-} (Yoshida et al., 1998), *Bak*^{-/-} (Lindsten et al., 2000), *Bax*^{-/-} (Lindsten et al., 2000), *Casp9*^{-/-} (Kuida et al., 1998), *Casp3*^{-/-} (Kuida et al., 1996), *Casp7*^{-/-} (Lakhani et al., 2006), *Irfar1*^{-/-} (Hwang et al., 1995), *Myd88*^{-/-} (Adachi et al., 1998), and *STING*^{-/-} (Jin et al., 2011) strains have been described. Animal procedures were approved by the Walter and Eliza Hall Institute Animal Ethics Committee.

Cell Death Assays

Cell death was induced by exposure to ABT-737 (AbbVie), Dexamethasone (Sigma), WEHI-539 (MedChemExpress), or Etoposide (Hospira). Where indicated, cells were preincubated for 1 hr with MRT-67307 (Sigma) and for 15–30 min with ABT-737, followed by continuous exposure to Q-VD-Oph (SM Biochemicals) or zVAD.fmk (R&D Systems). Cell viability was quantified by CellTiterGlo (Promega) or flow cytometric analysis of cells excluding 5 μ g/ml propidium iodide (PI) (Sigma) and, where indicated, cells also negative for AnnexinV-FITC (InvivoGen) binding using a FACSCalibur (BD) or LSRII (BD). Caspase activity was assayed by the addition of caspase3/7Glo (Promega) or by immunoblotting as described in the [Extended Experimental Procedures](#).

Measurement of IFN- β

IFN- β protein was measured using the VeriKine-HS Human or Mouse Interferon Beta ELISA (PBL Assay Science).

Generation of mtDNA-Depleted ρ^0 Cells

MEFs were cultured in Dulbecco's modified Eagle's medium (DMEM) (GIBCO) supplemented with 4 mM L-glutamine, 4.5 g/l glucose, 10% FCS, 100 μ g/ml sodium pyruvate, and 50 μ g/ml uridine as described (Hashiguchi and Zhang-Akiyama, 2009). 100 ng/ml ethidium bromide was added to the medium for 6–0 days. qPCR evaluation of mtDNA content by qPCR, transfection with Poly(I:C)(HMW)/LyoVec (InvivoGen), and expression profiling are described in [Extended Experimental Procedures](#).

Immunoprecipitation/PCR

Mcl1^{-/-} MEFs transduced with an expression plasmid (pMSCV-IRES-Hygro) encoding Flag-tagged mouse cGAS were treated with ABT-737 and Q-VD-Oph or left untreated. Following crosslinking of DNA and associated proteins, immunoprecipitation was performed with anti-FLAG M2 (Sigma) or mouse-IgG (BD) and coprecipitated DNA examined by real-time qPCR. Oligonucleotide sequences are listed in [Extended Experimental Procedures](#).

Statistics

Data and statistical methods are expressed as outlined in figure legends. Standard statistical methods were performed using Prism software (GraphPad). Bonferroni post hoc test was used to correct for multiple testing.

ACCESSION NUMBERS

The Gene Expression Omnibus accession numbers for the microarray data sets reported in this paper are GSE57934 and GSE59972.

SUPPLEMENTAL INFORMATION

Supplemental Information includes Extended Experimental Procedures, seven figures, and two tables and can be found with this article online at <http://dx.doi.org/10.1016/j.cell.2014.11.036>.

AUTHOR CONTRIBUTIONS

M.J.W. and B.T.K. designed research, analyzed data and wrote the paper. M.J.W., K.M., R.M.L., M.E.R., and D.M. performed research and analyzed data. D.C.S.H., J.C.C., M.F.v.D., G.L., M.J.H., and S.B. contributed vital reagents and insightful discussions.

ACKNOWLEDGMENTS

The authors thank J. Corbin and L. Di Rago for excellent technical assistance; K. Franks, E. Lanera, K. McGregor, S. Ross, K. Stoev, L. Wilkins, and E. Kryan for outstanding animal husbandry; S. Monard for expert flow cytometry assistance; T. Mak for *Apaf1*^{+/-} mice; R. Flavell for *Casp3*^{+/-} *Casp7*^{+/-} mice; C. Thompson for *Bak*^{+/-} and *Bax*^{+/-} mice; P. Crack for *Irfar1*^{+/-} mice; D. Fairlie and E. Lee for Bim variants; K. Aumann and C. De Nardo for manuscript assistance; and A. Strasser, J. Choi, S. Best, A. Rongvaux, and R. Flavell for insightful discussions. This work was supported by Project Grants (516725 and 575535), Program Grants (461219, 461221, and 1016647), Fellowships (D.C.S.H. and B.T.K.), and an Independent Research Institutes Infrastructure Support Scheme Grant (361646) from the Australian National Health and Medical Research Council; a scholarship from the Leukemia Foundation of Australia (M.J.W.), fellowships from the Cancer Council of Victoria (M.J.W. and D.M.); an Australian Postgraduate Award scholarship (K.M.); a fellowship from the Sylvia and Charles Viertel Foundation (B.T.K.); the Australian Cancer Research Fund; and a Victorian State Government Operational Infrastructure Support Grant.

Received: June 9, 2014

Revised: September 22, 2014

Accepted: November 10, 2014

Published: December 18, 2014

REFERENCES

- Adachi, O., Kawai, T., Takeda, K., Matsumoto, M., Tsutsui, H., Sakagami, M., Nakanishi, K., and Akira, S. (1998). Targeted disruption of the MyD88 gene results in loss of IL-1- and IL-18-mediated function. *Immunity* 9, 143–150.
- Barber, G.N. (2014). STING-dependent cytosolic DNA sensing pathways. *Trends Immunol.* 35, 88–93.
- Burguillos, M.A., Deierborg, T., Kavanagh, E., Persson, A., Hajji, N., Garcia-Quintanilla, A., Cano, J., Brundin, P., Englund, E., Venero, J.L., and Joseph, B. (2011). Caspase signalling controls microglia activation and neurotoxicity. *Nature* 472, 319–324.
- Cayrol, C., and Girard, J.-P. (2009). The IL-1-like cytokine IL-33 is inactivated after maturation by caspase-1. *Proc. Natl. Acad. Sci. USA* 106, 9021–9026.
- Chauvier, D., Ankri, S., Charriaut-Marlangue, C., Casimir, R., and Jacotot, E. (2007). Broad-spectrum caspase inhibitors: from myth to reality? *Cell Death Differ.* 14, 387–391.

- Civril, F., Deimling, T., de Oliveira Mann, C.C., Ablasser, A., Moldt, M., Witte, G., Hornung, V., and Hopfner, K.P. (2013). Structural mechanism of cytosolic DNA sensing by cGAS. *Nature* *498*, 332–337.
- Crawford, E.D., and Wells, J.A. (2011). Caspase substrates and cellular remodeling. *Annu. Rev. Biochem.* *80*, 1055–1087.
- Crawford, E.D., Seaman, J.E., Agard, N., Hsu, G.W., Julien, O., Mahrus, S., Nguyen, H., Shimbo, K., Yoshihara, H.A., Zhuang, M., et al. (2013). The DegraBase: a database of proteolysis in healthy and apoptotic human cells. *Mol. Cell Proteomics* *12*, 813–824.
- Dillon, C.P., Weinlich, R., Rodriguez, D.A., Cripps, J.G., Quarato, G., Gurung, P., Verbist, K.C., Brewer, T.L., Llambi, F., Gong, Y.-N., et al. (2014). RIPK1 blocks early postnatal lethality mediated by caspase-8 and RIPK3. *Cell* *157*, 1189–1202.
- Doitsh, G., Galloway, N.L.K., Geng, X., Yang, Z., Monroe, K.M., Zepeda, O., Hunt, P.W., Hatano, H., Sowinski, S., Muñoz-Arias, I., and Greene, W.C. (2014). Cell death by pyroptosis drives CD4 T-cell depletion in HIV-1 infection. *Nature* *505*, 509–514.
- Domen, J., Cheshier, S.H., and Weissman, I.L. (2000). The role of apoptosis in the regulation of hematopoietic stem cells: Overexpression of Bcl-2 increases both their number and repopulation potential. *J. Exp. Med.* *191*, 253–264.
- Ekert, P.G., Read, S.H., Silke, J., Marsden, V.S., Kaufmann, H., Hawkins, C.J., Gerl, R., Kumar, S., and Vaux, D.L. (2004). Apaf-1 and caspase-9 accelerate apoptosis, but do not determine whether factor-deprived or drug-treated cells die. *J. Cell Biol.* *165*, 835–842.
- Enari, M., Sakahira, H., Yokoyama, H., Okawa, K., Iwamatsu, A., and Nagata, S. (1998). A caspase-activated DNase that degrades DNA during apoptosis, and its inhibitor ICAD. *Nature* *391*, 43–50.
- Essers, M.A.G., Offner, S., Blanco-Bose, W.E., Waibler, Z., Kalinke, U., Duchosal, M.A., and Trumpp, A. (2009). IFN α activates dormant haematopoietic stem cells in vivo. *Nature* *458*, 904–908.
- Hashiguchi, K., and Zhang-Akiyama, Q.M. (2009). Establishment of human cell lines lacking mitochondrial DNA. *Methods Mol. Biol.* *554*, 383–391.
- Honarpour, N., Tabuchi, K., Stark, J.M., Hammer, R.E., Südhof, T.C., Parada, L.F., Wang, X., Richardson, J.A., and Herz, J. (2001). Embryonic neuronal death due to neurotrophin and neurotransmitter deprivation occurs independent of Apaf-1. *Neuroscience* *106*, 263–274.
- Huang, Q., Li, F., Liu, X., Li, W., Shi, W., Liu, F.-F., O'Sullivan, B., He, Z., Peng, Y., Tan, A.C., et al. (2011). Caspase 3-mediated stimulation of tumor cell repopulation during cancer radiotherapy. *Nat. Med.* *17*, 860–866.
- Hwang, S.Y., Hertzog, P.J., Holland, K.A., Sumarsono, S.H., Tymms, M.J., Hamilton, J.A., Whitty, G., Bertonecello, I., and Kola, I. (1995). A null mutation in the gene encoding a type I interferon receptor component eliminates anti-proliferative and antiviral responses to interferons alpha and beta and alters macrophage responses. *Proc. Natl. Acad. Sci. USA* *92*, 11284–11288.
- Irrinki, K.M., Mallilankaraman, K., Thapa, R.J., Chandramoorthy, H.C., Smith, F.J., Jog, N.R., Gandhirajan, R.K., Kelsen, S.G., Houser, S.R., May, M.J., et al. (2011). Requirement of FADD, NEMO, and BAX/BAK for aberrant mitochondrial function in tumor necrosis factor alpha-induced necrosis. *Mol. Cell Biol.* *31*, 3745–3758.
- Janzen, V., Fleming, H.E., Riedt, T., Karlsson, G., Riese, M.J., Lo Celso, C., Reynolds, G., Milne, C.D., Paige, C.J., Karlsson, S., et al. (2008). Hematopoietic stem cell responsiveness to exogenous signals is limited by caspase-3. *Cell Stem Cell* *2*, 584–594.
- Jin, L., Hill, K.K., Filak, H., Mogan, J., Knowles, H., Zhang, B., Perraud, A.L., Cambier, J.C., and Lenz, L.L. (2011). MPYS is required for IFN response factor 3 activation and type I IFN production in the response of cultured phagocytes to bacterial second messengers cyclic-di-AMP and cyclic-di-GMP. *J. Immunol.* *187*, 2595–2601.
- Kazama, H., Ricci, J.-E., Herndon, J.M., Hoppe, G., Green, D.R., and Ferguson, T.A. (2008). Induction of immunological tolerance by apoptotic cells requires caspase-dependent oxidation of high-mobility group box-1 protein. *Immunity* *29*, 21–32.
- King, M.P., and Attardi, G. (1989). Human cells lacking mtDNA: repopulation with exogenous mitochondria by complementation. *Science* *246*, 500–503.
- Kuida, K., Zheng, T.S., Na, S., Kuan, C., Yang, D., Karasuyama, H., Rakic, P., and Flavell, R.A. (1996). Decreased apoptosis in the brain and premature lethality in CPP32-deficient mice. *Nature* *384*, 368–372.
- Kuida, K., Haydar, T.F., Kuan, C.Y., Gu, Y., Taya, C., Karasuyama, H., Su, M.S., Rakic, P., and Flavell, R.A. (1998). Reduced apoptosis and cytochrome c-mediated caspase activation in mice lacking caspase 9. *Cell* *94*, 325–337.
- Labi, V., Bertele, D., Woess, C., Tischner, D., Bock, F.J., Schwemmers, S., Pahl, H.L., Geley, S., Kunze, M., Niemeyer, C.M., et al. (2013). Haematopoietic stem cell survival and transplantation efficacy is limited by the BH3-only proteins Bim and Bmf. *EMBO Mol. Med.* *5*, 122–136.
- Lakhani, S.A., Masud, A., Kuida, K., Porter, G.A., Jr., Booth, C.J., Mehal, W.Z., Inayat, I., and Flavell, R.A. (2006). Caspases 3 and 7: key mediators of mitochondrial events of apoptosis. *Science* *311*, 847–851.
- Lee, E.F., Czabotar, P.E., van Delft, M.F., Michalak, E.M., Boyle, M.J., Willis, S.N., Puthalakath, H., Bouillet, P., Colman, P.M., Huang, D.C., and Fairlie, W.D. (2008). A novel BH3 ligand that selectively targets Mcl-1 reveals that apoptosis can proceed without Mcl-1 degradation. *J. Cell Biol.* *180*, 341–355.
- Li, P., Nijhawan, D., Budihardjo, I., Srinivasula, S.M., Ahmad, M., Alnemri, E.S., and Wang, X. (1997). Cytochrome c and dATP-dependent formation of Apaf-1/caspase-9 complex initiates an apoptotic protease cascade. *Cell* *91*, 479–489.
- Li, F., He, Z., Shen, J., Huang, Q., Li, W., Liu, X., He, Y., Wolf, F., and Li, C.Y. (2010a). Apoptotic caspases regulate induction of iPSCs from human fibroblasts. *Cell Stem Cell* *7*, 508–520.
- Li, Z., Jo, J., Jia, J.M., Lo, S.C., Whitcomb, D.J., Jiao, S., Cho, K., and Sheng, M. (2010b). Caspase-3 activation via mitochondria is required for long-term depression and AMPA receptor internalization. *Cell* *141*, 859–871.
- Lindsten, T., Ross, A.J., King, A., Zong, W.X., Rathmell, J.C., Shiels, H.A., Ulrich, E., Waymire, K.G., Mahar, P., Frauwirth, K., et al. (2000). The combined functions of proapoptotic Bcl-2 family members bak and bax are essential for normal development of multiple tissues. *Mol. Cell* *6*, 1389–1399.
- Linkermann, A., and Green, D.R. (2014). Necroptosis. *N. Engl. J. Med.* *370*, 455–465.
- Lüthi, A.U., Cullen, S.P., McNeela, E.A., Durie, P.J., Afonina, I.S., Sheridan, C., Brumatti, G., Taylor, R.C., Kersse, K., Vandenabeele, P., et al. (2009). Suppression of interleukin-33 bioactivity through proteolysis by apoptotic caspases. *Immunity* *31*, 84–98.
- Marsden, V.S., O'Connor, L., O'Reilly, L.A., Silke, J., Metcalf, D., Ekert, P.G., Huang, D.C., Cecconi, F., Kuida, K., Tomaselli, K.J., et al. (2002). Apoptosis initiated by Bcl-2-regulated caspase activation independently of the cytochrome c/Apaf-1/caspase-9 apoptosome. *Nature* *419*, 634–637.
- Martin, S.J., Henry, C.M., and Cullen, S.P. (2012). A perspective on mammalian caspases as positive and negative regulators of inflammation. *Mol. Cell* *46*, 387–397.
- Mcllwain, D.R., Berger, T., and Mak, T.W. (2013). Caspase functions in cell death and disease. *Cold Spring Harb. Perspect. Biol.* *5*, a008656.
- Moujalled, D.M., Cook, W.D., Okamoto, T., Murphy, J., Lawlor, K.E., Vince, J.E., and Vaux, D.L. (2013). TNF can activate RIPK3 and cause programmed necrosis in the absence of RIPK1. *Cell Death Dis.* *4*, e465.
- Nonomura, K., Yamaguchi, Y., Hamachi, M., Koike, M., Uchiyama, Y., Nakazato, K., Mochizuki, A., Sakaue-Sawano, A., Miyawaki, A., Yoshida, H., et al. (2013). Local apoptosis modulates early mammalian brain development through the elimination of morphogen-producing cells. *Dev. Cell* *27*, 621–634.
- O'Brien, T., and Dixit, V.M. (2009). Drug discovery in apoptosis. In *Encyclopedia of Life Sciences*. Published online December 15, 2009. <http://dx.doi.org/10.1002/9780470015902.a0021587>.
- Oltersdorf, T., Elmore, S.W., Shoemaker, A.R., Armstrong, R.C., Augeri, D.J., Belli, B.A., Bruncko, M., Deckwerth, T.L., Dinges, J., Hajduk, P.J., et al. (2005). An inhibitor of Bcl-2 family proteins induces regression of solid tumours. *Nature* *435*, 677–681.

- Opferman, J.T., Iwasaki, H., Ong, C.C., Suh, H., Mizuno, S., Akashi, K., and Korsmeyer, S.J. (2005). Obligate role of anti-apoptotic MCL-1 in the survival of hematopoietic stem cells. *Science* 307, 1101–1104.
- Oppenheim, R.W., Flavell, R.A., Vinsant, S., Prevette, D., Kuan, C.Y., and Rakic, P. (2001). Programmed cell death of developing mammalian neurons after genetic deletion of caspases. *J. Neurosci.* 21, 4752–4760.
- Orelia, C., and Dzierzak, E. (2007). Bcl-2 expression and apoptosis in the regulation of hematopoietic stem cells. *Leuk. Lymphoma* 48, 16–24.
- Paludan, S.R., and Bowie, A.G. (2013). Immune sensing of DNA. *Immunity* 38, 870–880.
- Prinz, M., and Knobloch, K.-P. (2012). Type I interferons as ambiguous modulators of chronic inflammation in the central nervous system. *Front. Immunol.* 3, 67.
- Sato, T., Onai, N., Yoshihara, H., Arai, F., Suda, T., and Ohteki, T. (2009). Interferon regulatory factor-2 protects quiescent hematopoietic stem cells from type I interferon-dependent exhaustion. *Nat. Med.* 15, 696–700.
- Shimada, K., Crother, T.R., Karlin, J., Dagvadorj, J., Chiba, N., Chen, S., Ramanujan, V.K., Wolf, A.J., Vergnes, L., Ojcius, D.M., et al. (2012). Oxidized mitochondrial DNA activates the NLRP3 inflammasome during apoptosis. *Immunity* 36, 401–414.
- Sun, L., Wu, J., Du, F., Chen, X., and Chen, Z.J. (2013). Cyclic GMP-AMP synthase is a cytosolic DNA sensor that activates the type I interferon pathway. *Science* 339, 786–791.
- Suzuki, J., Denning, D.P., Imanishi, E., Horvitz, H.R., and Nagata, S. (2013). Xk-related protein 8 and CED-8 promote phosphatidylserine exposure in apoptotic cells. *Science* 341, 403–406.
- Thapa, R.J., Nogusa, S., Chen, P., Maki, J.L., Lerro, A., Andrade, M., Rall, G.F., Degtarev, A., and Balachandran, S. (2013). Interferon-induced RIP1/RIP3-mediated necrosis requires PKR and is licensed by FADD and caspases. *Proc. Natl. Acad. Sci. U.S.A.* 110, E3109–E3118.
- van Delft, M.F., Wei, A.H., Mason, K.D., Vandenberg, C.J., Chen, L., Czabotar, P.E., Willis, S.N., Scott, C.L., Day, C.L., Cory, S., et al. (2006). The BH3 mimetic ABT-737 targets selective Bcl-2 proteins and efficiently induces apoptosis via Bak/Bax if Mcl-1 is neutralized. *Cancer Cell* 10, 389–399.
- van Delft, M.F., Smith, D.P., Lahoud, M.H., Huang, D.C.S., and Adams, J.M. (2010). Apoptosis and non-inflammatory phagocytosis can be induced by mitochondrial damage without caspases. *Cell Death Differ.* 17, 821–832.
- Wei, M.C., Zong, W.X., Cheng, E.H., Lindsten, T., Panoutsakopoulou, V., Ross, A.J., Roth, K.A., MacGregor, G.R., Thompson, C.B., and Korsmeyer, S.J. (2001). Proapoptotic BAX and BAK: a requisite gateway to mitochondrial dysfunction and death. *Science* 292, 727–730.
- Yi, C.H., and Yuan, J. (2009). The Jekyll and Hyde functions of caspases. *Dev. Cell* 16, 21–34.
- Yoshida, H., Kong, Y.Y., Yoshida, R., Elia, A.J., Hakem, A., Hakem, R., Penninger, J.M., and Mak, T.W. (1998). Apaf1 is required for mitochondrial pathways of apoptosis and brain development. *Cell* 94, 739–750.
- Youle, R.J., and Strasser, A. (2008). The BCL-2 protein family: opposing activities that mediate cell death. *Nat. Rev. Mol. Cell Biol.* 9, 47–59.

EXTENDED EXPERIMENTAL PROCEDURES

Automated Blood Counts

Peripheral blood was collected from the retro-orbital plexus into Microtainer tubes containing EDTA (Sarstedt). Complete and differential blood cell counts were determined using an Advia 120 automated hematological analyzer (Bayer).

Bioplex Cytokine Assay

The measurement of 23 cytokines was performed using the Bio-plex (Biorad) luminex fluorescent bead array according to the manufacturer's instructions. Data were analyzed using the Bio-plex Manager 6.0 Software (Biorad).

Chimeras and Transplantation Analysis

Chimeras were generated by transplanting lethally irradiated male CD45.1⁺ recipients with 10⁶ CD45.2⁺ E13.5 fetal liver cells. For serial transplants, 2 × 10⁶ bone marrow cells from primary recipients, 16 weeks post-transplant, were intravenously injected into lethally irradiated CD45.1⁺ secondary recipients. At 16 weeks post-transplant, donor contribution was analyzed by flow cytometry on an LSRII (BD) for multi-lineage representation of the CD45.2⁺ marker. For competitive transplants, CD45.1⁺ recipients were reconstituted with 1 × 10⁶ CD45.2⁺ test and CD45.1⁺CD45.2⁺ competitor fetal liver cells in a 1:1 ratio. At 16 weeks post-transplant, contribution of donor and test cells was assessed by flow cytometry.

Culture of Primary Hematopoietic Cells

Whole blood was obtained through the generous support of healthy donors on the Walter and Eliza Hall Institute Volunteer Donor Registry. Peripheral blood mononuclear cells (PBMCs) were isolated from whole blood by Ficoll gradient. Cells were cultured in Iscove's Modified Dulbecco's Media (IMDM) supplemented with 10% heat-inactivated fetal calf serum (FCS) at 37°C, 10% CO₂. This procedure complied with regulatory standards, and was approved by The Walter and Eliza Hall Institute Human Research Ethics Committee. Single cell suspensions of primary mouse splenocytes were obtained from whole tissue, and red blood cells removed by hypotonic lysis. Cells were then cultured in Dulbecco's Modified Eagle's medium (DME) supplemented with 10% heat-inactivated FCS at 37°C, 5% CO₂.

Culture of Mouse Embryonic Fibroblasts

Mouse embryonic fibroblasts (MEFs) were from mice on a C57BL/6 background or backcrossed for more than ten generations. MEFs from embryonic day (E)13–14 embryos were made following the removal of the head, thoracic cavity, and fetal liver, and a single cell suspension was seeded in DME medium (GIBCO) supplemented with 4 mM L-glutamine, 4.5 g/l glucose and 10% heat-inactivated FCS in 0.1% gelatin tissue culture plates at 37°C, 5% CO₂. Immortalization of MEFs was performed by transfection (Amaxa Nucleofector) of an expression plasmid encoding the SV40 T antigen (a gift from D. Huang). To generate *Mcl1*^{-/-} MEFs, immortalized *Mcl1*^{fl/fl} MEFs were transiently transfected (Amaxa Nucleofector) with an expression plasmid encoding Cre recombinase (pEF-Cre-IRES-Neo). Single cell-derived clones were screened for response to ABT-737 and knockout confirmed by immunoblot. Expression plasmids encoding Bim_s2A or Bim_s4E have been previously described (Lee et al., 2008). For viral transduction of MEFs with Bim_s2A or Bim_s4E, expression plasmids were transiently transfected into Phoenix ecotropic packaging cells by Fugene 6 (Roche) or calcium-phosphate transfection. Viral supernatants were used to infect cells. MEFs were maintained in DME medium (GIBCO) supplemented with 4 mM L-glutamine, 4.5 g/l glucose and 10% heat-inactivated FCS at 37°C, 5% CO₂.

CRISPR/Cas9-Mediated Gene Targeting in MEFs

To generate knockout MEFs by CRISPR/Cas9-mediated gene targeting, a Cas9 expression plasmid and a small guide RNA (sgRNA) expression plasmid was used (B.J. Aubrey, G.L. Kelly, A. Kueh, M.S. Brennan, L. O'Connor, L. Milla, S. Wilcox, L. Tai, A. Strasser, and M.J.H., unpublished data; further information and request for the lentiviral plasmids should be directed to herold@wehi.edu.au). Targeting guide sequences were designed using the Optimized CRISPR Design Tool from the Zhang Laboratory-MIT (crispr.mit.edu), and guide oligos were annealed and ligated into the sgRNA vector. To generate lentivirus, 293T cells were transfected by Fugene 6 (Roche) with packaging plasmids (pMDLg/pRRE and pRSV-Rev) and an envelope plasmid (pCMV-VSVG). Immortalized *WT* MEFs were infected with viral supernatants. Single cell clones were derived and CRISPR/Cas9-mediated InDel production (generated from one guide-RNA per gene) in the targeted gene was confirmed by Sanger Sequencing. Additionally, *Irf3*^{CRISPR-/-} and *cGAS*^{CRISPR-/-} single cell-derived clones were functionally tested by assessing IFN-β production in response to transfection with interferon-stimulatory DNA (ISD) (InvivoGen). The targeting guide sequences are listed under Oligonucleotides.

DNA Laddering

Analysis of DNA laddering is described elsewhere (Gong et al., 1994).

Histology

Tissues were collected in 10% buffered formalin and embedded in paraffin before being sectioned and mounted onto glass slides. Sections were stained with hematoxylin and eosin for histological examination. Images were acquired using the Nikon Eclipse

E600 microscope, AxioCam Hrc (Carl Zeiss MicroImaging) and AxioVersion 3.1 image acquisition software (Carl Zeiss MicroImaging).

Imaging

PicoGreen staining for imaging mtDNA has been described previously (Ashley et al., 2005). Briefly, cells were plated in 8 well chamber slides and incubated with 3 μ l/ml PicoGreen dye (InvivoGen) in serum-free media for 1 hr at 37°C, followed by Mitotracker Red-FM dye (InvivoGen) (1 μ M). Wells were washed in phosphate-buffered saline (PBS), before phenol red-free media was added and cells imaged on the Zeiss LSM 780 confocal microscope using a 63x/1.4 Plan Apo objective. Images shown are maximum intensity projections from Z-stacks.

Immunoblotting

Cell lysates were made using TNKE buffer (50 mM Tris pH 7.5, 120 mM NaCl, 2 mM KCl, 2 mM EDTA, 1% Triton X-100, supplemented with complete protease inhibitor cocktail (Roche)), or KALB buffer (1% Triton X-100, 150 mM NaCl, 50 mM Tris pH 7.5, 1 mM EDTA, 1 mM phenylmethylsulfonyl fluoride, 0.1 mM Na₃VO₄, supplemented with complete protease inhibitor cocktail) and spun clear of the insoluble fraction. Supernatants were quantified by Bradford assay (BioRad), then boiled in SDS reducing buffer. Samples were run through 4%–12% Bis-Tris gels (InvivoGen) and transferred to nitrocellulose membranes via dry-transfer using the iBlot system (InvivoGen). Membranes were blocked for 1 hr in Odyssey Buffer (Li-Cor) before incubation with primary antibodies: Bak (Sigma #B5897), Bax (WEHI MabLab clone 49F9-13-3), HSP70 (in-house), active-caspase-3 (Chemicon #AB3623), FLAG (in-house, 9H1). Secondary antibodies were acquired from Rockland (#610-132-121) and Molecular Probes (#A-21001MP, #A-21906). Membranes were visualized using Odyssey system (Li-Cor).

Microarray Analysis

RNA was labeled, amplified and hybridized to Illumina Mouse WG6 V2.0 Expression BeadChips in triplicate by the Australian Genome Research Facility. The GenomeStudio summary probe profile was analyzed in R (R Development Core Team, 2013) using the limma package (Smyth, 2005). Expression values were background adjusted, quantile normalized (Shi et al., 2010) and log₂ transformed. These data have been deposited in the Gene Expression Omnibus under the accession number GSE57934 and GSE59972. Probes with low expression (detection p-value < 0.95 across all arrays) or poor annotation (Barbosa-Morais et al., 2010) were removed from further analysis. Linear models with array weights (Ritchie et al., 2006) were fitted to summarize over the replicate samples. Contrasts between the different genotypes or cell treatments were estimated within each experiment, and differential expression assessed using moderated *t*-statistics (Smyth, 2004). Probes were ranked according to their false discovery rate (FDR), and those with a FDR < 0.05 were considered differentially expressed.

Microarray Analysis: Gene Set Enrichment Analysis

Analysis of the c2 gene signatures from MSigDB (Subramanian et al., 2005), and ChrM, was performed using Camera (Wu and Smyth, 2012) to look for up- or downregulated gene sets. Human gene signatures were converted to mouse by matching Entrez Gene IDs between species using the Jackson Laboratory Homology and Orthology reports (as described at <http://bioinf.wehi.edu.au/software/MSigDB/index.html>).

Real-Time qPCR

For analysis of mtDNA content, total DNA was isolated from cells with a DNeasy blood and tissue kit (QIAGEN). Real-time qPCR was used for measurement of mtDNA depletion using primers for the mitochondrial genes *ND1* and *ND5* and the nuclear gene *POLG*. The mitochondrial genes were normalized to that of nuclear and compared to untreated cells to calculate the percentage of depletion. For analysis of gene expression, total RNA was isolated with RNeasy Mini kit (QIAGEN). Reverse transcription was performed using oligo(dT) primer and SuperScript III reverse transcriptase (Life Technologies) according to the manufacturer's instructions and genomic DNA was removed by Dnase I treatment (QIAGEN). Real-time qPCR was carried out on a Rotor-Gene RG-6000 (Corbett) or on a Light-Cycler 480 (Roche) using SensiMix SYBR kit (Quantace) under the following conditions: 10 min at 95°C, followed by 40 cycles of 15 s at 95°C, 20 s at 62°C, and 20 s at 72°C. For Rotor-Gene analysis, gene expression was determined using the Rotor-Gene software version 1.7. For LightCycler 480 analysis, gene expression was determined using the $\Delta\Delta$ CT method. The primer sequences are listed under Oligonucleotides.

Oligonucleotides

Gene	Oligonucleotide Sequence	mtDNA*	gDNA*
<i>gapdh</i>	tgacatcaagaaggtggtgaagc	-	-
<i>gapdh</i>	aaggtggaagagtgggagttgctg		

(Continued on next page)

Continued

Gene	Oligonucleotide Sequence	mtDNA*	gDNA*
<i>Ifnb1</i>	ggaagattgacgtgggaga	-	-
<i>Ifnb1</i>	ccttgcaccctccagtaat		
<i>Ifnb1</i>	ttacactgccttgccatcc	-	-
<i>Ifnb1</i>	actgtctgctggaggatcat		
<i>Irf7</i>	tgcagtacagccacatactgg	-	-
<i>Irf7</i>	ctcgtaaacacggctcttgctc		
<i>Oas2</i>	ctgtggctgaaaatccatga	-	-
<i>Oas2</i>	ctgtgagaactcccctggtg		
<i>POLG</i>	gatgaatgggcctaccttga	-	1
<i>POLG</i>	tgggctcctgtttctacagc		
<i>POLG</i>	tcctggaacagttgtgcttc	-	2
<i>POLG</i>	ccatctactcaggacggagttc		
<i>atp6</i>	ccataaatctaagtatagccattccac	1	-
<i>atp6</i>	agcttttagttgtgctggaag		
<i>nd1</i>	caaacactattacaaccaagaaca	2	-
<i>nd1</i>	tcatattatggctatgggtcagg		
<i>nd2</i>	ccatcaactcaatctcactctatg	3	-
<i>nd2</i>	gaatcctgttagtggtggaagg		
<i>nd5</i>	agcattcgaagcatctttg	4	-
<i>nd5</i>	ttgtgaggactggaatgctg		
<i>nd5</i>	ccacgattcttcaagcta	5	-
<i>nd5</i>	tcggatgtctgttctgctg		
<i>nd6</i>	tggttgggagattggtg	6	-
<i>nd6</i>	cacaactatataatgccgtaccc		
<i>mr1</i>	cctctagggttgtaaatttcg	7	-
<i>mr1</i>	cgaagataattagttgggtaaatcg		
<i>mr2</i>	aaacagctttaaccattgtaggc	8	-
<i>mr2</i>	ttgagcttgaacgctttcttta		
<i>CAD</i> guide	gccacatgccggcgatcc	-	-
<i>cGAS</i> guide	tgttaaactggaagtcccc	-	-
<i>Irf3</i> guide	ataagccggacgtgcaacc	-	-

*mtDNA and gDNA amplicons related to immunoprecipitation/PCR experiments.

SUPPLEMENTAL REFERENCES

Ashley, N., Harris, D., and Poulton, J. (2005). Detection of mitochondrial DNA depletion in living human cells using PicoGreen staining. *Exp. Cell Res.* 303, 432–446.

Barbosa-Morais, N.L., Dunning, M.J., Samarajiwa, S.A., Darot, J.F., Ritchie, M.E., Lynch, A.G., and Tavaré, S. (2010). A re-annotation pipeline for Illumina BeadArrays: improving the interpretation of gene expression data. *Nucleic Acids Res.* 38, e17.

Gong, J., Traganos, F., and Darzynkiewicz, Z. (1994). A selective procedure for DNA extraction from apoptotic cells applicable for gel electrophoresis and flow cytometry. *Anal. Biochem.* 218, 314–319.

R Development Core Team (2013). A language and environment for statistical computing (Vienna: R Foundation for Statistical Computing).

Ritchie, M.E., Diyagama, D., Neilson, J., van Laar, R., Dobrovic, A., Holloway, A., and Smyth, G.K. (2006). Empirical array quality weights in the analysis of microarray data. *BMC Bioinformatics* 7, 261.

- Shi, W., Oshlack, A., and Smyth, G.K. (2010). Optimizing the noise versus bias trade-off for Illumina whole genome expression BeadChips. *Nucleic Acids Res.* *38*, e204.
- Smyth, G.K. (2004). Linear models and empirical bayes methods for assessing differential expression in microarray experiments. *Stat. Appl. Genet. Mol. Biol.* *3*, Article3.
- Smyth, G.K. (2005). limma: linear models for microarray data. In *Bioinformatics and Computational Biology Solutions Using R and Bioconductor*, R. Gentleman, V. Carey, W. Huber, R. Irizarry, and S. Dudoit, eds. (New York: Springer), pp. 397–420.
- Subramanian, A., Tamayo, P., Mootha, V.K., Mukherjee, S., Ebert, B.L., Gillette, M.A., Paulovich, A., Pomeroy, S.L., Golub, T.R., Lander, E.S., and Mesirov, J.P. (2005). Gene set enrichment analysis: a knowledge-based approach for interpreting genome-wide expression profiles. *Proc. Natl. Acad. Sci. USA* *102*, 15545–15550.
- Wu, D., and Smyth, G.K. (2012). Camera: a competitive gene set test accounting for inter-gene correlation. *Nucleic Acids Res.* *40*, e133.

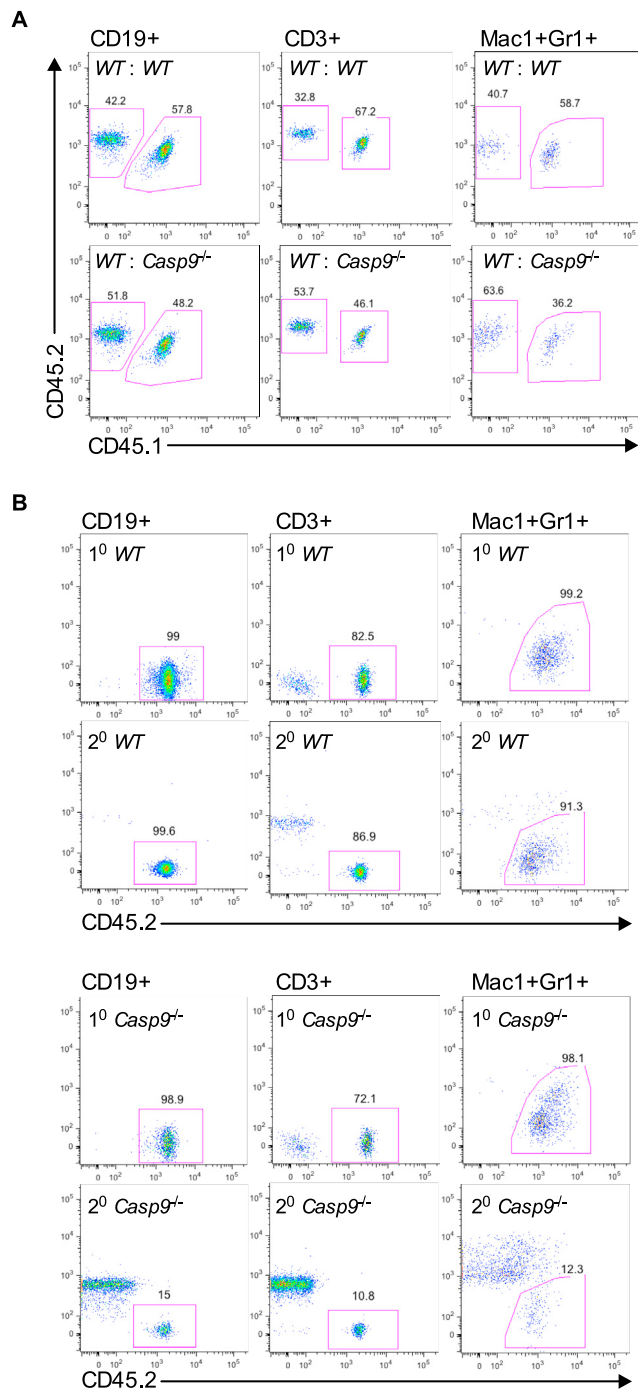


Figure S1. Representative Analysis of Peripheral Blood Chimerism, Related to Figure 1

(A) FACS plots of test (CD45.2⁺) and competitor (CD45.1⁺CD45.2⁺) contribution to peripheral blood B cell (CD19⁺), T cell (CD3⁺) and myeloid cell (Mac1⁺Gr1⁺) lineages from competitive fetal liver transplant recipients at 16 weeks post-transplant.

(B) FACS plots of donor (CD45.2⁺) contribution to peripheral blood B cell (CD19⁺), T cell (CD3⁺) and myeloid cell (Mac1⁺Gr1⁺) lineages in primary (1[°]) and secondary (2[°]) transplant recipients at 16 weeks post-transplant.

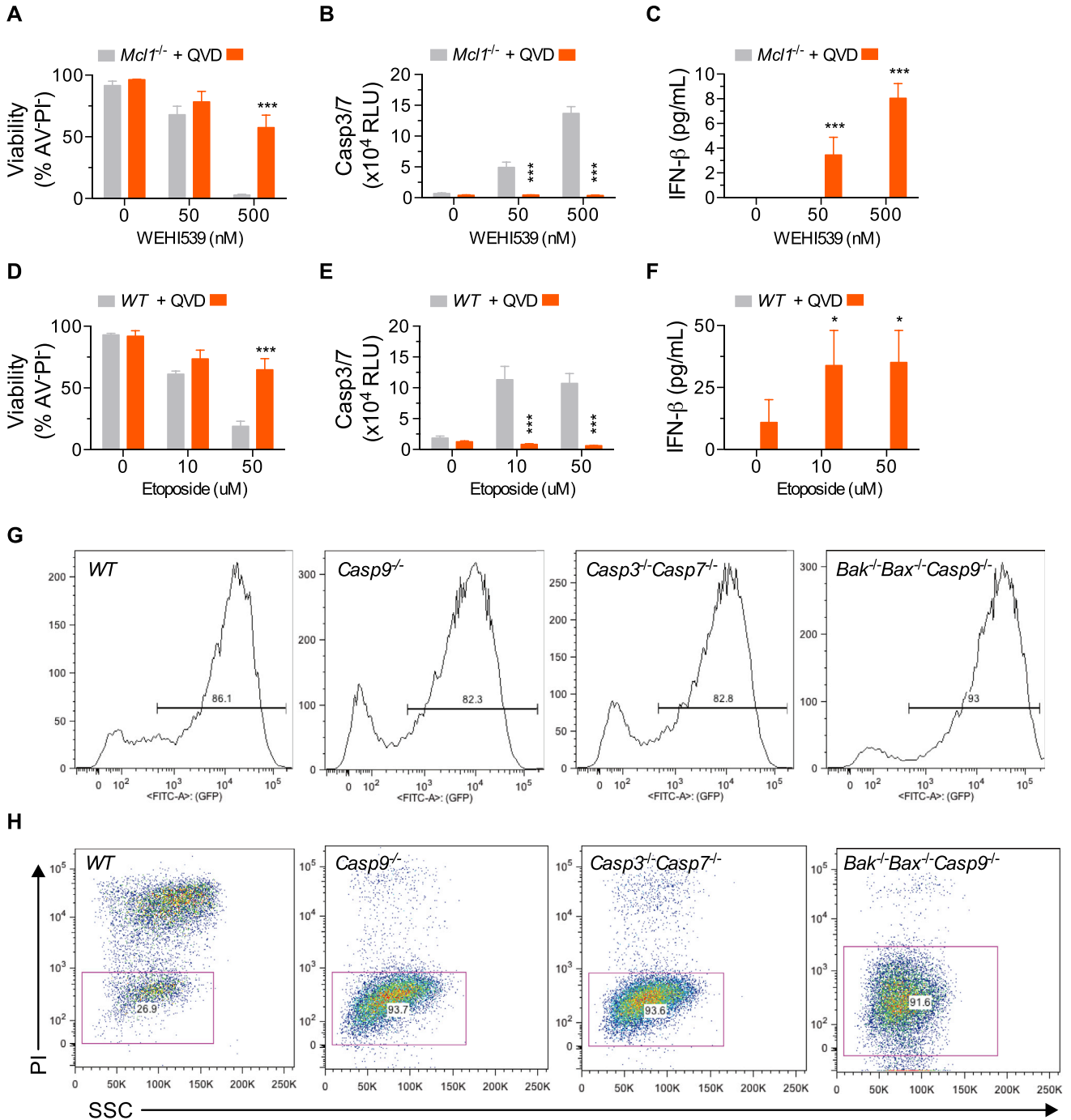


Figure S2. Multiple Apoptotic Stimuli Induce Type I Interferon Production When Caspases Are Inhibited, Related to Figure 5

(A-C) (A) Bar graphs of the viability of MEFs treated with WEHI-539 and co-incubated with 20-30 uM of Q-VD-Oph (QVD) for 24 hr (B) caspase activity after 6 hr and (C) IFN-β in supernatant after 24 hr. (n = 3 independent MEF lines).

(D-F) (D) Bar graphs of the viability of MEFs treated with Etoposide and co-incubated with 20-30 uM of Q-VD-Oph (QVD) for 24 hr (E) caspase activity after 24 hr and (F) IFN-β in supernatant after 24 hr. (n = 3 independent MEF lines).

(G) Representative infection efficiency for one mouse MEF line of each genotype transduced with an expression vector encoding Bim_{2A}-GFP.

(H) Plots of the viability of MEFs in (G) treated with ABT-737 (500 nM) for 20 hr. Gates display propidium iodide (PI) negative viable cells.

Means were compared using a two-tailed t test. Data represent the mean ± SEM. *p ≤ 0.05, **p ≤ 0.01, ***p ≤ 0.005.

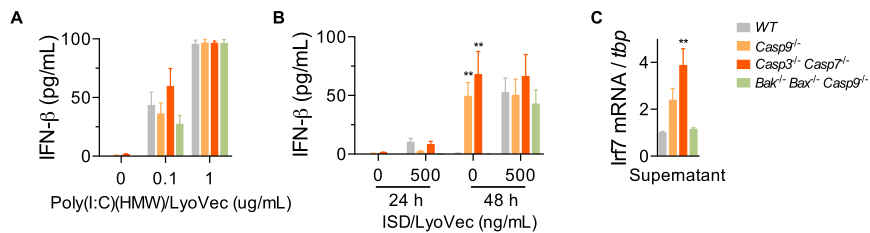


Figure S3. Characterization of Type I Interferon Production from WT, *Casp9*^{-/-}, *Casp3*^{-/-} *Casp7*^{-/-}, and *Bak*^{-/-} *Bax*^{-/-} *Casp9*^{-/-} MEFs, Related to Figure 5

(A) Bar graph of IFN- β in the supernatant of MEFs 24 hr after transfection with Poly(I:C)(HMW). (n = 3 independent MEF lines per genotype).

(B) Bar graph of IFN- β in the supernatant of MEFs transfected with interferon-stimulating DNA (ISD) for the indicated time. (n = 3 independent MEF lines per genotype).

(C) Real-time qPCR analysis of *Irf7* mRNA expression in WT MEFs 12 hr after the addition of supernatant from untreated MEFs of the indicated genotype. (n = 3 independent MEF lines per genotype, supernatant transferred to 2 WT MEF lines).

Means were compared to WT using a one-way ANOVA with Bonferroni correction. Data represent the mean \pm SEM. *p \leq 0.05, **p \leq 0.01, ***p \leq 0.005.

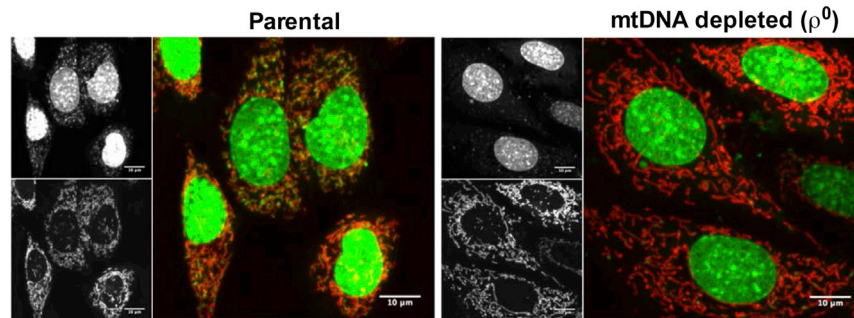


Figure S4. Confocal Analysis of mtDNA Depletion, Related to Figure 6

Representative images of *Mcl1*^{-/-} (left) and mtDNA depleted ρ^0 *Mcl1*^{-/-} (right) MEFs. Images shown are maximum intensity projections of z-stack images. Black and white images show single stains: DNA stain PicoGreen (top panel) and mitochondrial stain MitoTracker Red (bottom panel), directly beside the corresponding overlaid image in color.

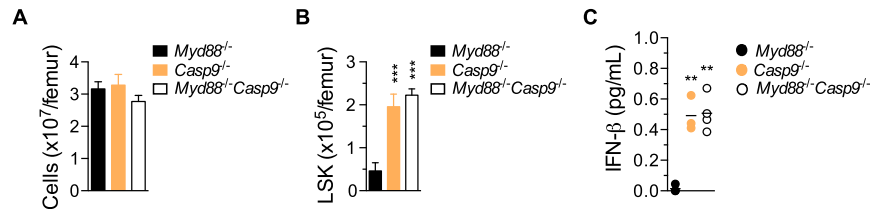


Figure S5. Deletion of Myd88 Does Not Prevent Type I IFN Production in *Casp9*^{-/-} Bone Marrow Chimeras, Related to Figure 7

(A) Bone marrow cellularity from *Myd88*^{-/-} (n = 3), *Casp9*^{-/-} (n = 4) and *Myd88*^{-/-} *Casp9*^{-/-} (n = 6) bone marrow chimeras, 10-12 weeks post-transplant.

(B) Number of donor-derived LSK cells from *Myd88*^{-/-} (n = 3), *Casp9*^{-/-} (n = 4) and *Myd88*^{-/-} *Casp9*^{-/-} (n = 6) bone marrow chimeras, 10-12 weeks post-transplant.

(C) IFN- β protein in serum of *Myd88*^{-/-} (n = 3), *Casp9*^{-/-} (n = 3) and *Myd88*^{-/-} *Casp9*^{-/-} (n = 4).

Means were compared to WT using a one-way ANOVA with Bonferroni correction. Data represent the mean \pm SEM. *p \leq 0.05, **p \leq 0.01, ***p \leq 0.005.

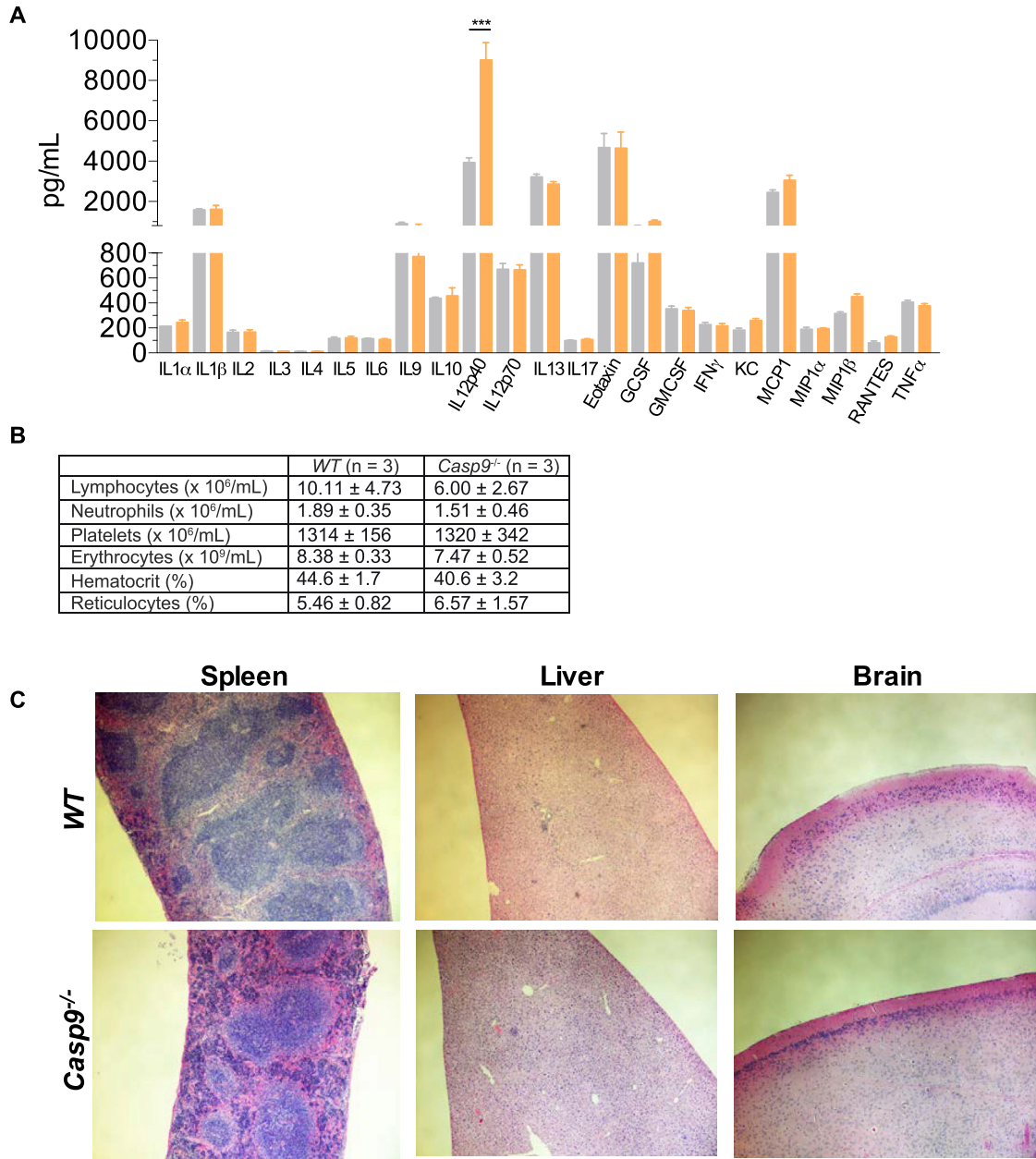


Figure S6. Absence of Inflammation in Casp9^{-/-} Bone Marrow Chimeras, Related to Figure 7

(A) Serum cytokine profile from WT and Casp9^{-/-} mice 10-12 weeks post-transplant measured by Bio-plex. (n = 10-12 mice per genotype).

(B) Automated blood count from WT and Casp9^{-/-} mice 52 weeks post transplant.

(C) Hematoxylin and eosin stained sections from spleen, liver and brain of WT and Casp9^{-/-} mice 52 weeks post transplant. Original magnification x200. Means were compared to WT using a two-tailed t test. Data represent the mean ± SEM. *p ≤ 0.05, **p ≤ 0.01, ***p ≤ 0.005.

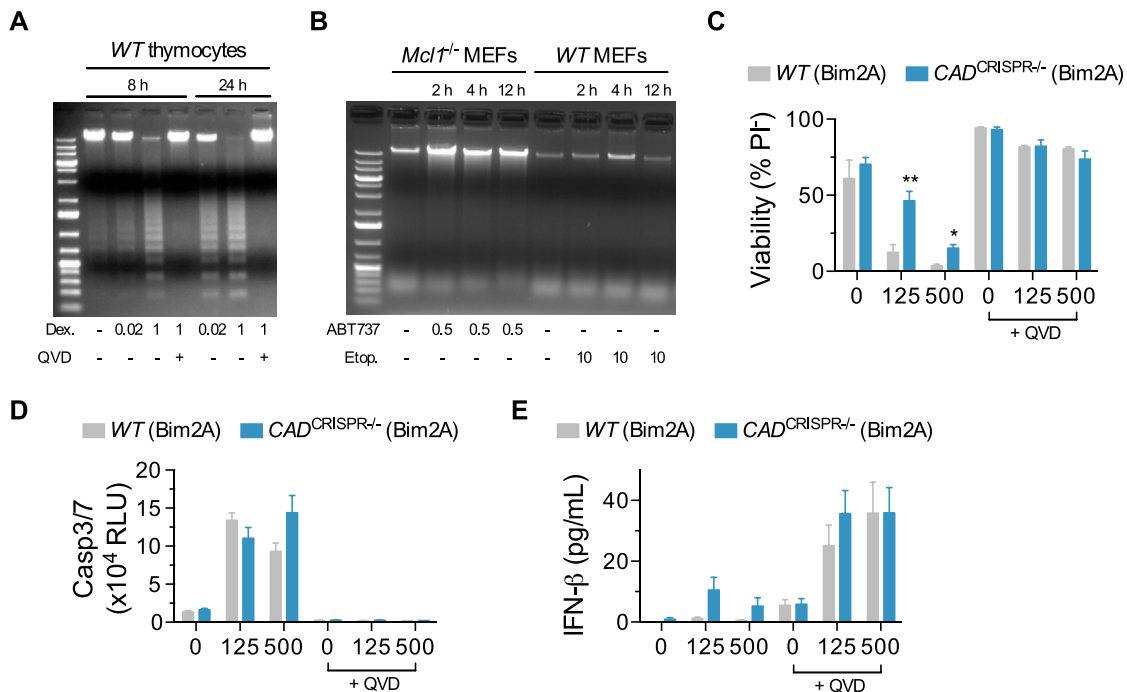


Figure S7. Role of CAD in the Suppression of Type I Interferon Production by Active Caspases, Relates to Figure 7

(A) DNA laddering in thymocytes treated with Dexamethasone (Dex.) (uM) or co-incubated with 20-30 uM of Q-VD-Oph (QVD) for the indicated time.

(B) DNA laddering in *Mcl1*^{-/-} MEFs treated with ABT-737 (uM) and *WT* MEFs treated with Etoposide (Etop.) (uM) for the indicated time.

(C) Bar graphs of the viability of MEFs expressing Bim_s2A and treated with ABT-737 for 24 hr and (D) caspase activity after 6 hr (E) IFN-β in supernatant after 24 hr. (n = 5 independent CRISPR/Cas9-targeted MEF clones and 2 independent *WT* MEF lines).

Means were compared to *WT* using a two-tailed t test. Data represent the mean ± SEM. *p ≤ 0.05, **p ≤ 0.01.